EdVidParse: Detecting People and Content in Educational Videos

by

Michele Pratusevich

S.B., Massachusetts Institute of Technology (2013)

Submitted to the Department of Electrical Engineering and Computer Science

in partial fulfillment of the requirements for the degree of

Masters of Engineering in Computer Science and Engineering

at the

MASSACHUSETTS INSTITUTE OF TECHNOLOGY

June 2015

Author . . . .
Department of Electrical Engineering and Computer Science
May 22, 2015

Certified by . . . .
Robert C. Miller
Professor, Department of Electrical Engineering and Computer Science
Thesis Supervisor

Certified by . . . .
Antonio Torralba
Associate Professor, Department of Electrical Engineering and Computer Science
Thesis Supervisor

Accepted by . . . .
Albert Meyer
Chairman, Department Committee on Graduate Theses

EdVidParse: Detecting People and Content in Educational Videos

by

Michele Pratusevich

Submitted to the Department of Electrical Engineering and Computer Science
on May 22, 2015, in partial fulfillment of the
requirements for the degree of
Masters of Engineering in Computer Science and Engineering

Abstract

There are thousands of hours of educational content on the Internet, with services like edX, Coursera, Berkeley WebCasts, and others offering hundreds of courses to hundreds of thousands of learners. Consequently, researchers are interested in the effectiveness of video learning. While educational videos vary, they share two common attributes: people and textual content. People are presenting content to learners in the form of text, graphs, charts, tables, and diagrams. With an annotation of people and textual content in an educational video, researchers can study the relationship between video learning and retention. This thesis presents EdVidParse, an automatic tool that takes an educational video and annotates it with bounding boxes around the people and textual content. EdVidParse uses internal features from deep convolutional neural networks to estimate the bounding boxes, achieving a 0.43 AP score on a test set. Three applications of EdVidParse, including identifying the video type, identifying people and textual content for interface design, and removing a person from a picture-in-picture video are presented. EdVidParse provides an easy interface for identifying people and textual content inside educational videos for use in video annotation, interface design, and video reconfiguration.

Thesis Supervisor: Robert C. Miller
Title: Professor, Department of Electrical Engineering and Computer Science

Thesis Supervisor: Antonio Torralba
Title: Associate Professor, Department of Electrical Engineering and Computer Science

Acknowledgments

To those at MIT supporting my work: this work would not have been possible by the generosity of Rob Miller and the entire User Interface Design group at CSAIL - Carrie Cai, Juho Kim, Elena Glassman, and Max Goldman. They took me in when I was looking for a project and have been supportive ever since. Antonio Torralba and the Vision group also took me in and let me participate in some of the most innovative computer vision research happening at MIT. Thanks to Rebecca Krosnick for putting up with bad early prototypes. And thanks to Bryt Bradley for always smiling whenever I walk in the door.

To those who made MIT possible: thanks to my parents, Tatyana and Gennady, who encouraged me in the pursuits of my dreams, and have to put up with my taste for adventure. And of course, thanks to my ever-supporting boyfriend Robin, who is always a loving, snarky sounding board.

Contents

Chapter 1

Introduction

Educational video content on the Internet is increasing at an exponential rate. In November 2014, 182 courses were offered on edX (`edx.org`), with over 1000 hours of video content. By June 2015, 516 courses were offered with over 6000 hours of video. Other massively open online course (MOOC) providers like Coursera (`coursera.org`) and Udacity (`udacity.com`) offer more than 1000 courses each at any given time. YouTube is the most common video hosting and distribution platform, with the recent YouTube EDU initiative hosting over 700,000 educational videos.

With this influx of content, researchers are interested in analyzing the effectiveness of video learning. This includes exploring the relationship between video composition and student engagement, and exploring alternate ways of presenting videos to learners at different stages of the learning process. For example, systems that effectively summarize videos or automatically extract slides can be beneficial for skimming or reviewing, while reconfiguring videos for fast playback can be good for initial viewing.

While educational videos vary, most share two common attributes: people and textual content. People are presenting material, performing an experiment, and providing a face to a new content. Textual content makes up the bulk of educational video material - graphs, tables, charts, images, formulas, and text present information. The composition of people and content in videos can give information about the type of video being watched. For example, if there is less textual content, the video is more likely about a topic from the humanities. Or if the size of the person relative to the rest of the frame is small, the video is more likely a classroom recording. Videos where a lecturer's head features prominently are more engaging for learners [18]. Being able to effectively identify people and textual content in videos can be a useful tool in analyzing educational videos.

Computer vision techniques for analyzing images and videos have drastically improved in the last few years with the increasing use of neural networks, improving performance in vision tasks such as object detection and scene classification. The structure of an educational video is relatively consistent (when was the last time you saw a tropical beach scene in a traditional classroom recording?), so computer vision techniques specifically tuned for educational video applications can be effective.

This work develops a computer vision pipeline called EdVidParse for identifying people and regions of salient textual content inside a video. EdVidParse[1] finds people and textual content such as graphs, text, and drawings inside video frames. It also classifies the frame into a scene or composition type - for example whether it is a classroom-recorded lecture, a studio recording, or a synthetically-created image. These annotations allow researchers to answer questions related to the prevalence of people and textual content in educational videos. EdVidParse turns a video into a JSON annotation in near-real-time, taking about one second of processing per second of video. Alternative approaches to object detection in videos can be more accurate, but EdVidParse trades off some accuracy in exchange for speed.

This work also presents a dataset of object and composition annotations specifically in educational videos for training and testing models that achieved a mean average precision (AP) of 0.437 for object detection and 86 percent classification accuracy for scene classification. EdVidParse uses a new approach for training bounding box estimators using internal neural network features.

Three applications of EdVidParse are presented as case studies: automatically annotating videos by production style, detecting people and content bounding boxes for a textbook-like video interface, and reconfiguring a picture-in-picture video into a video of just slides.

[1]Code can be found at `https://github.com/uid/ed-vid-parse`

Chapter 2

Related work

2.1 Educational videos

Because more students are learning online and through video, researchers are interested in maximizing the effectiveness of these videos by exploring video composition, summarization, and content extraction techniques. Questions about which types of videos are more engaging, or how to make videos useful to learners after they have already been initially watched, are critical to increasing the effectiveness of online learning.

Guo et. al. [18] explores the relationship between video production style and student engagement. Videos from 4 courses were classified into 6 types of production styles, or composition: slides, code (a demo being worked through), Khan-style (formulas being incrementally derived without seeing a person), classroom (a recorded lecture video), studio, and office desk. The study classified each video into a particular category, not taking into account videos that changed styles, say from a close-up of an instructor's face to a Khan-style derivation. The researchers found that videos with high production value, namely shooting videos in a special video production studio, did not result in greater student engagement and therefore might not be worth the money. The production styles proposed by Guo are a way of labeling a video in terms of composition, used as a foundation for the video style classification discussed in Section 4.1. Having a system that can automatically classify each frame of a video into a production style can allow faster data collection and more granular video analysis for engagement studies.

Eye-tracking studies with learners correlate learning with video frame content, with the goal of giving advice to content creators about effective video strategies. These studies show that it is easier for students to look at uncluttered text on a slide [35] and that students prefer watching videos with an instructor's face, even if it does not increase recall of the material [25]. To perform these studies, each pixel of the frame needs to be labeled as belonging to a few groups, like person, background, or text material, and is usually done by drawing outlines of objects in the frame by the researcher. Having a technique that can automatically annotate objects to be manually fixed can save time for researchers performing further studies.

If classroom lectures are recorded and posted to the web, a problem is that lecturers often stand in front of relevant notes on a blackboard. While giving a classroom lecture, this is less of a problem, since students can ask for clarification when needed. However, this is not ideal in an online environment, where there is not the guarantee of a community that can answer questions. Instead of the lecturer changing their presentation style, alternate means of recording classroom lectures such as EduCase [20] present systems that work with the normal flow of classroom instruction. The EduCase system records an instructor in a classroom with multiple cameras and a depth sensor, automatically removing the lecturer from in front of the blackboard notes and reconfiguring the video to present both the lecturer and the notes in one video stream that is ready to post online. Being able to remove a lecturer from a video can make a recorded video more suitable for an online environment.

Because MOOCs are offered online to a massive audience, the data from student clicks, watches, rewinds, etc. provides an estimate of learner engagement with a particular video. Kim et. al. [23] aggregate student interaction data and correlate it with specific points in videos to understand why interaction peaks happen. For example, students tend to re-watch sections of video where the lecturer speaks too fast, or they tend to skip over longer boring sections. Being able to annotate more videos with video composition data can give more clues about the reasons behind some interaction peaks.

Meanwhile, a goal of the Berkeley Video Digests system [32] is to provide an interface for effectively skimming a video or finding a point of interest. Much like chapter headings in books, Video Digests uses a combination of automatic, manual, and crowdsourced techniques to split an educational video into sections that can then be combined with a transcript in a skimmable format. Improving the automatic sectioning techniques can offer improvements for students reviewing material, since the current system does not take video composition into account.

Other crowd-sourced methods attempt to give section headings to video segments specifically in how-to videos [43]. These videos have a natural progression of steps, making it easier to verify with a crowd and offering natural breakpoints throughout the video. It is possible that clues within the video itself can offer a starting point for these section-level annotations.

In addition to summarization, the video watching interface can be combined with sectioning and transcripts to give the student a more granular view of a video, such as in the VideoDoc interface [28]. A lecturer can then design the video interface without the constraints of a single, linear experience by combining two potential video streams and lecture notes or transcripts in the same page. Sections are naturally broken up by video type, so a segment with a lecturer's head might be followed by a segment with just a slide. Being able to automatically annotate textual content and lecturer's head in the videos can save the lecturer work in splitting up the video view.

Another problem for learners with online videos is searching within a video for a relevant section. Text-based OCR solutions are common, using text displayed in the video as a description of what is happening inside the video itself. Yang et. al. [45] extract as much text as possible from the videos and apply OCR, so textual keywords can be used to search within a video. Yu et. al. [47] take this approach further to index an entire video with a set of keywords extracted from OCR on the intra-video text. While this approach works well for videos with high textual content, videos that rely on a lecturer speaking or doing a demonstration may benefit from visual cues within the videos. There is no way for a learner to search within a video based on purely visual cues.

To solve the problem of video discovery, the Talkminer project [1] tries to aggregate educational videos into one search engine. Specifically, the focus is on extracting full-frame lecture slides from talks that are OCR'ed and indexed into a custom search engine. Users can then search for specific keywords that will return full videos around the desired slide to provide contextual information. The limitations are that videos with heavy blackboard work or slides that appear smaller in the frame are not indexed well.

Building further on the slide extraction idea, Wang et. al. [42] and Kayal et. al. [22] both take advantage of the similar structure in traditional lecture slides to further semantically extract information or build pages of notes from lectures. As lecturers become more innovative in their slide presentations, or even use them less frequently in their lecture videos, these approaches will be important for indexing previously-posted videos, and the techniques used by Wang and Kayal can be applied to videos with similar structure. However, a more general framework is needed for extracting content from general online educational videos.

Because researchers are interested in answering questions that relate to video structure, they can all benefit from being able to automatically annotate videos with areas of textual content and areas where people occur. These video annotations can help in answering questions about student engagement and help in designing interfaces for students interacting with videos.

2.2 Object detection and scene recognition

Parsing the visual structure of an educational video relies on a number of computer vision techniques that were developed in literature in the more general case. Techniques have been developed to solve a variety of tasks with high speed and accuracy:

- **object recognition** - Classify an image of a single object into an object class, like dog, desk, book, etc. Features are first extracted from the image, then classified. Standard benchmarks include the ImageNet database [6].

- **object detection** - For an image, find bounding boxes around all instances of a given object class in that image. Standard benchmarks include the PASCAL database [11].

- **scene recognition** - Classify an image into a scene category, such as classroom, beach, office, etc. Standard benchmarks include the SUN database [44].

EdVidParse does both object detection and scene recognition - it detects people and textual content in videos, in addition to classifying video frames into video production style.

Hand-crafted features that rely on interest points in an image such as corners performed well at computer vision tasks until neural networks became popular. Features such as histograms of oriented gradients (HOG) [5] and SIFT [30] for static images and spatio-temporal features for video [26] perform well in ideal conditions, but are not robust to lighting changes, object occlusion, and viewpoint change. Part-based models attempt to account for these shortcomings by relying on a mix of parts for an object - so for example a person can be detected even if only his legs are seen. Scene recognition suffered the same shortcomings with the use of GIST features [31] - the features were not very robust to changes in viewpoint, lighting, or occlusion. Because educational videos are different enough in lighting and viewpoint, especially when trying to find people in the videos, more general features extracted from neural networks were used instead of hand-crafted features.

For object detection, an additional challenge is estimating the bounding box where an object occurs. Early approaches simply generated all possible image subregions and performed image classification on each region separately. A key improvement over exhaustive sliding-window search approaches was the idea of using non-maximal suppression to filter out high-scoring detections that significantly overlap previously-detected regions [13]. While this technique was originally used as part of a person classifier using part-based models, it is now generally used in all object detection tasks. EdVidParse relies heavily on object detection methods to find people and content effectively in video frames.

Instead of exhaustive enumeration of all possible object boxes, the idea of generating a set of object proposals, or regions where there is a high probability of finding an object, were developed. An object proposal algorithm should have high recall - the correct detection should be in the set of boxes it produces - but it can generate as many extra boxes as necessary, since classification will be performed on each object proposal anyway. Methods such as selective search [41] and edge boxes [50] are used to generate object proposals. These methods take advantage of the observation that a box with an object in it has a high density of edges inside the box. EdVidParse uses edge boxes and the associated code [7, 8, 50] for generating object proposals, notably in the R-CNN comparison described in Section 5.1.

For the classification step in all computer vision tasks, there are a number of available methods, with support vector machines (SVMs) being the most commonly used. SVM classification and training is done using the Liblinear (for linear kernels) and LibSVM (for other kernels) libraries [4, 12]. Typically grid search is used for finding a set of acceptable SVM parameters. This project uses the Spearmint[1] package for hyperparameter selection, such as misclassification tolerance and bias [15, 36, 37, 38, 40]. Spearmint takes advantage of Bayesian optimization techniques to estimate optimal hyperparameters for a task, removing the need for arbitrary grid search for optimal parameters and decreasing training time. The best-performing algorithms on the PASCAL and SUN datasets use SVMs for classification, so EdVidParse uses this approach as well.

Another advantage of SVMs are that hard negative mining can be used to increase accuracy [13, 39]. In hard negative mining, an SVM classifier is initially trained with a dataset, then incrementally improved with negative examples. For example, say an SVM classifier is trained to identify whether the image is a dog or not. It is initially trained with 100 positive examples of dogs and 100 negative examples of dogs. To improve the accuracy of the classifier, thousands of random image crops from 1000 images known to not have any dogs in them are generated, and features are extracted from all those image crops. These negative examples are classified with the original

[1]`https://github.com/HIPS/Spearmint`

classifier, and those that are incorrectly classified are added as negative examples to the training set. This way, an initial classifier is incrementally improved only with negative examples it misclassifies.

Because EdVidParse is an object detection pipeline, techniques such as object proposals and classification with SVMs are key components to its effectiveness.

2.3 Convolutional neural networks (CNNs)

All the records set using hand-crafted features for computer vision tasks were overtaken by the use of convolutional neural nets (CNNs). The ImageNet Large-Scale Visual Recognition Challenge (ILSVRC) is an annual object recognition challenge where participants had to assign one of 1000 classes to a particular image of an object, and is often used as a performance benchmark for any new methods developed. In 2012, a team submitted an entry that beat all previous performance benchmarks in ILSVRC by nearly 20 percentage points, using convolutional neural networks as the basis for an object classifier [27]. Trained on more than a million images, this network learns more complex representations of images than was previously possible. The network architecture proposed in this 2012 ILSVRC entry became the standard in computer vision for any computer vision tasks and has been dubbed AlexNet. Since then, all winning entries in the ILSVRC have been CNN-based [34]. The basic principle of a convolutional neural network is that an image is fed through a series of learned convolutional filters layered on top of each other.

Network training end-to-end is achieved quickly using backpropagation [33] over millions of example images as training data. Additionally, the discovery and widespread use of rectified linear units (ReLUs) instead of sigmoid activation functions for neuron activations has led to better results at train and test time, according to Krizhevsky, et. al. [27]. Sigmoid activation functions, used in the neocognitron [14] (the precursor to neural networks) and in logistic regression classifiers, follow a sigmoid function, whereas ReLU activation functions look like a hockey stick, as shown in Figure 2-1. This means that when ReLUs are used, each individual activation is greater than or equal to zero, with each positive value scaling linearly for that activation. This leads to more stability during training time, and the property that each neuron only lets through positive predictive values, rather than values that indicate absence. The use of ReLUs allows for the bounding box estimation procedure described in Section 3.1.3.

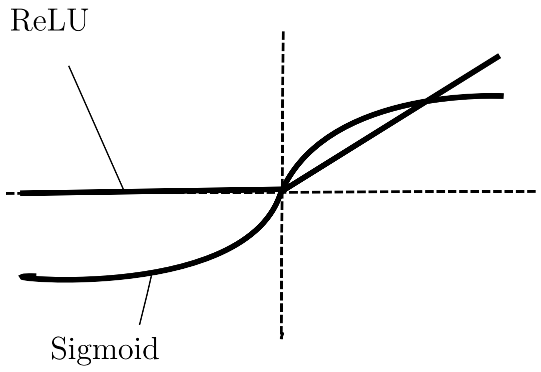

Figure 2-1: A comparison of the rectified linear unit (ReLU) and sigmoid activation functions

During training, because the errors from the training set are propagated through the network through back-propagation, this is called a backwards pass through the network. During the testing or feature extraction phase, an image is simply forward-passed through the network, performing the convolution and addition operations according to the learned parameters, but without propagating errors back through the network. EdVidParse takes advantage of fast forward passes through the network to extract features.

2.3.1 AlexNet

LeCun et. al. proposed using backpropagation and stochastic gradient descent in CNNs for hand-written digit recognition in the 1980s [29], and AlexNet built on these early ideas. But the success of CNNs until 2012 was mostly hindered by processing power and efficiency of training, so once this barrier was crossed, the effectiveness of using CNNs for vision tasks greatly increased.

AlexNet was so successful and revolutionary at the ILSVRC that the starting-point reference network architecture used by many research computer vision systems exactly copies that of AlexNet. The network architecture is shown in Figure 2-2, and the sizes of the internal network outputs are shown in Table 2.1. Layers always take as input the output of the layers beneath them rather than the original image, so the resultant convolution can be complicated to understand. However, taking the result of a single $n \times n$ output in a given layer, called a unit, can provide insight about the contents of an image, as proposed by Zhou, et. al. [48], and discussed in Section 3.1.3. Each unit is composed of individual activations - responses of a particular activation to an image patch.

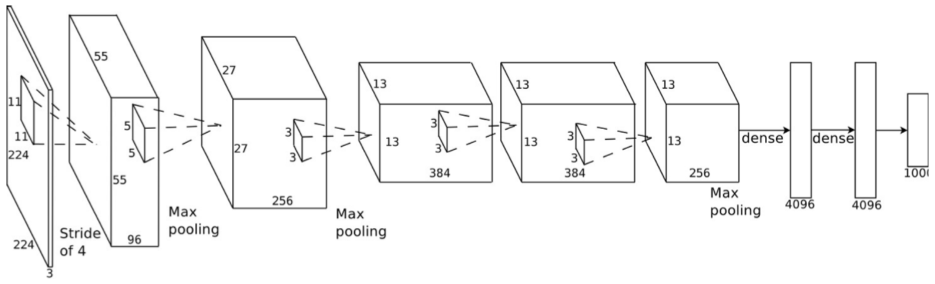

Figure 2-2: AlexNet neural network architecture used in feature extraction. Taken from Krizhevsky et. al. [27].

The three most common layer types in these neural networks are *convolutional* (conv) layers, *pooling* (pool) layers, and *fully connected* (fc) layers. A convolutional layer takes an image patch and performs a convolution on it according to some learned parameters. The resulting outputs taken together are the units for that network layer. For example, the *conv1* layer outputs 96 different units, all of size 55×55, computed by taking a series of convolution on image patches. Later convolutional layers perform the convolutions on activations of the units below them, not directly on an image patch. A pooling layer takes as input a number of activations and performs an operation on the activations to reduce the dimensionality. AlexNet uses max-pooling layers, which take as input the activations from the layer below it and outputs the maximum activation from the layer below. In this way, only the strongest activations are propagated forward through the network, reducing the number of parameters that need to be learned and the amount of data to be propagated through the system. Other types of pooling include average-pooling and min-pooling, but AlexNet uses

	Layer	Total output size	No. of units	Activations
2D units	conv1	$55 \times 55 \times 96$	96	290400
	pool1	$27 \times 27 \times 96$	96	69984
	conv2	$27 \times 27 \times 256$	256	186624
	pool2	$13 \times 13 \times 256$	256	43264
	conv3	$13 \times 13 \times 384$	384	64896
	conv4	$13 \times 13 \times 384$	384	64896
	conv5	$13 \times 13 \times 256$	256	43264
	pool5	$6 \times 6 \times 256$	256	9216
1D units	fc6	$1 \times 1 \times 4096$		4096
	fc7	$1 \times 1 \times 4096$		4096
	fc8	$1 \times 1 \times 1000$		1000
Total			1984	781736

Table 2.1: Output sizes of intermediate layers in the AlexNet reference network

max-pooling and this technique has become standard in deep network learning. Fully-connected layers simply compute a linear function as a result of their inputs, like in the neocognitron or linear logistic regression. The standard AlexNet architecture has 5 convolutional layers, 3 pooling layers, and 3 fully-connected layers. Typically, the output of the top layer in any network (fc8 in the case of AlexNet) is a vector of probabilities that perform the task the network was trained to do. In the case of AlexNet, the task was classification of an image into 1000 classes, so the fc8 layer has 1000 outputs representing the probability of belonging to each of these 1000 classes. The algorithm discussed for bounding box estimation in Section 3.1.3 takes advantage of the properties of each type of network layer.

The Caffe software [21] makes training, testing, and using neural networks efficient and easy. The standard AlexNet reference model, along with a number of other network models, are freely distributed online in the Caffe format, making development and testing straightforward. Because Caffe is open source, it is easy to distribute the final EdVidParse system online.

2.3.2 Improvements on AlexNet

After the success of AlexNet in the ILSVRC, CNNs were shown to be useful as general feature extractors [2, 9, 10, 46]. In general this is accomplished by passing an image through the network, and instead of looking at the output fc8 layer, the fc7 layer (which has 4096 output values) would effectively transform an image into a vector of 4096 values that can then be fed into any kind of classification, regression, or other system for tasks such as classification, bounding box estimation, image segmentation, and others.

As an extension to CNNs, the Region-CNN (R-CNN) algorithm was developed to be competitive at the object detection task. The basic idea is to use detected regions from an object proposal algorithm as inputs to the neural network, accomplishing both object detection and object recognition simultaneously [16]. The goal of the object proposal algorithm is to identify regions in an image that are likely to contain an object, reducing the task of exhaustive search using a set of heuristics.

It has also been shown that using a baseline network like AlexNet and fine-tuning it for a specific task such as scene recognition is effective and cuts down on training time [17, 49]. The increase in performance from fine-tuning AlexNet for scene recognition outperformed the previous record set the use of hand-crafted features, as shown by Zhou et. al. [49]. Zhou publicly distributes two networks - PlacesCNN and HybridplacesCNN, that have been fine-tuned from AlexNet for scene recognition and combined scene-object recognition respectively. Fine-tuning a neural network for a set of images or classes that it was not originally trained to do is called domain adaptation. In this work, fine-tuning was performed on a small set of scene-labeled images with the PlacesCNN network as a base [49], described in Section 4.1.4.

The biggest obstacles with using deep learning for computer vision tasks are the large amount of data needed for effective network training, long training times (often requiring multiple GPUs and complex CUDA code), and finding the optimal set of hyperparameters that govern learning. This work takes advantage of pre-trained networks that, when combined with a limited amount of training data for a specific domain, can be used to achieve good results. Whenever possible, hyperparameters for learning rates and model selection were chosen based on parameters used by other researchers.

Recently, internal network units were shown to correlate with specific object detectors [48]. The main idea is that in networks trained for scene recognition, specific units act as object detectors, with the upper layers of the network synthesizing this information together to produce a final scene label. For example, in the PlacesCNN network, unit 3 in the conv5 layer activates in image regions containing faces. Because the main function of EdVidParse is detection of people and textual content (both are objects), this idea is used to find person and text units in deep networks. These units, most-studied in conv5 and pool5 layers, can be transformed into a mask on the image to serve as an estimator for object recognition. We heavily take advantage of this observation and develop a framework for constructing bounding box detection estimates using these internal features, detailed in Section 3.1.3.

2.4 Evaluation metrics

A number of metrics such as cross-validation accuracy, classification accuracy, precision, recall, F1 score, and AP score, can be used to evaluate object detection and scene recognition metrics, each with costs and benefits. For evaluation in this work we choose to use classification accuracy for scene recognition and AP score for object detection.

Cross-validation accuracy is used primarily for classification or recognition tasks. In n-fold cross-validation, a training set is divided into n groups, with each subset of $n-1$ subgroups used for training and the last group used for testing. The cross-validation accuracy is the average of the correct classification percentage from all the test sets. With multiple classes, the mean cross-validation accuracy is the mean of all the cross-validation accuracies among all classes. This metric has the advantage that it gives a good estimate of test accuracy, since the hold-one-out approach simulates real data. Additionally, cross-validation can be a way of simulating more data, since

$n-1$ classifiers can be trained and averaged instead of 1. However, this metric does not take into account unbalanced training sets. For example, if a training set of 100 images only has 3 examples of class A and 97 examples of class B, it is trivial to achieve 97 percent accuracy by always guessing class B as the predicted label, no matter the train-test split. Even if the class labels were divided equally among training and testing splits, the high accuracy can be misleading.

Classification accuracy is simply a measure of the percentage of correct classifications in a set of test labels. To combat class label imbalances, the test set should be equal in all class labels. This way a 75 percent classification accuracy for one class is comparable across all class labels.

Precision and recall can be used in evaluating object detection. For a given item in the test set, it is either a positive or negative example of a particular class C. A true positive is therefore an item in the test set that is both a member of C and is identified as a member of C. A false positive is an item identified as class C but is in fact not in class C. Precision is the ratio of true positives to true and false positives, measuring how good the false positive rate is:

$$\text{precision} = \frac{\text{true positives}}{\text{true positives} + \text{false positives}} \tag{2.1}$$

If a detection system achieves 100 percent precision (or a precision of 1), it means that all the objects identified as class C are in fact of class C, but it is not guaranteed that all objects of class C were found.

By contrast, recall is the ratio of true positives to true positives and false negatives, measuring the retrieval rate of the algorithm:

$$\text{recall} = \frac{\text{true positives}}{\text{true positives} + \text{false negatives}} \tag{2.2}$$

An algorithm with 100 percent recall (or a recall of 1) finds all instances of class C, but is not guaranteed to find only those items. To trivially achieve 100 percent recall, all possible items are identified as members of class C.

Because a classification algorithm wants to have both high accuracy and high recall, the harmonic mean of precision and recall, or the F1 score can be used:

$$\text{F1} = 2 \cdot \frac{\text{precision} \cdot \text{recall}}{\text{precision} + \text{recall}} \tag{2.3}$$

However, the drawback of this metric is that F1 only takes into account a specific value of precision and recall - rather than the relationship of precision and recall at different values. At 100 percent recall, there might only be 20 percent precision. But at 50 percent precision there can be 100 percent recall. Because there is a specific relationship between precision and recall, it makes sense to use a metric that takes into account all pairs of precision and recall values.

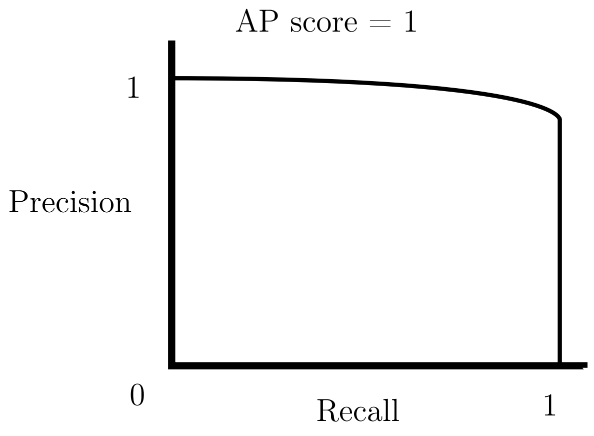

Figure 2-3: An ideal precision-recall curve with AP = 1

The AP score (or average precision) of a detector takes into account the relationship between precision and recall. Average precision is defined as the area under the precision-recall curve. An ideal detector has an AP score of 1, with a precision-recall curve like shown in Figure 2-3. This curve is calculated by ordering the predicted results by highest confidence and their corresponding correct labels, thresholding at various values, and plotting the precision and recall at those thresholds. The more that a precision-recall curve looks like this ideal, the better the detector. Instead of looking at the precision-recall graph to determine effectiveness, the AP score is used. The AP score metric has the advantage of taking into account all points on the precision-recall curve.

Classification accuracy is the same metric for multiclass problems - it has the same meaning as for one-class classification problems. To extend the AP score metric to multiclass problems, the AP score for each class separately is averaged to compute a mean AP score for the detector.

For scene recognition, test set accuracy is used, as is standard for multiclass classification problems. For object detection, AP score is used for both model selection and final evaluation [24]. This is consistent with the metrics used in computer vision literature for both classification and object detection.

Chapter 3

EdVidParse

3.1 System overview

EdVidParse is composed of two main pieces - the feature extractor and the feature processor. The feature extractor turns a video into a set of numerical features, and the feature processor either performs classification or bounding box estimation and outputs computer-readable JSON.

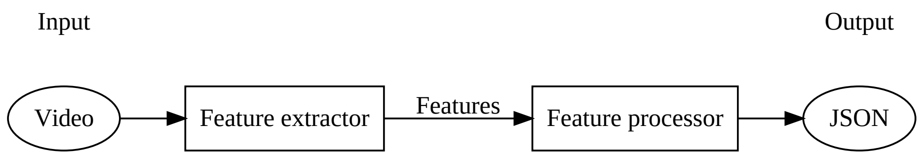

Figure 3-1: High-level system diagram for the video parsing tool

EdVidParse is written in Python, making it easy to quickly make changes to any part of the pipeline. The feature extractor that uses neural networks uses the open-source Caffe library [21] for efficient feature extraction and for ease of development. The feature processor uses the Liblinear and LibSVM libraries for classification [4, 12], and a custom-written interface for bounding box estimation.

There are two main tasks EdVidParse can accomplish - classification of a video frame into a style, such as pure slide, picture-in-picture, classroom lecture, etc., and detection of people and textual content in a video frame.

3.1.1 Design goals

EdVidParse has three main design goals:

- **Accuracy** - EdVidParse must be accurate enough to require minimal manual adjustment. Without working fast, there is no reason for a researcher to use a tool that accomplishes the same task that can be done more accurately by hand.

- **Speed** - Small accuracy tradeoffs in exchange for speed are acceptable. For a tool to be used, it must work reliably enough to need only minor manual adjustments.

- **Trainability** - A tool that can be re-trained with new video data will be more robust to changes in the future.

3.1.2 CNN feature extractor

The purpose of the feature extractor is to decompose the input video into frames, then extract image features from each of those frames (see Figure 3-2). While all video frames can be extracted from a video, in practice approximately one in every five frames are used for feature extraction. This is because adjacent frames in high-frame-rate videos do not change appreciably, but can instead cause noisy results later in the pipeline.

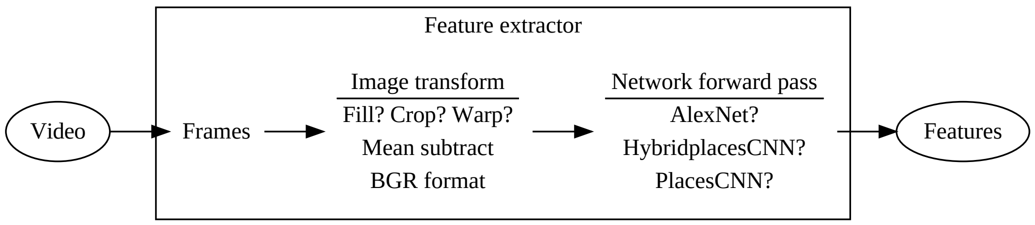

Figure 3-2: System diagram for feature extractor

Before the image is sent through the network, it goes through a pre-processing step where the image is converted from RGB-space to BGR-space and resized to 227×227

pixels, since this is the input type AlexNet requires. Additionally, the training image mean (a standard image distributed with AlexNet) is subtracted. When images are not square, there is a choice of *cropping*, *filling*, or *warping* the images to transform them to 227×227. Cropping finds the largest centered square piece of the image and scales it to the appropriate size. Filling scales the image as-is so that the largest dimension fits, then fills in the rest of the space with black pixels. Warping just resizes the image without any cropping or filling. Filling and cropping preserves in-image ratios, but objects appear smaller and can be harder to detect. Warping utilizes the entirety of both the original image and the final 227×227 area. Figure 3-3 shows the difference between the three pre-processing methods. Generally, the method chosen is warping, as standard with the original AlexNet, except in specific situations, as discussed in Section 3.2. With every rescaling operation there is a choice with the kind of pixel interpolation to use - nearest neighbor, bilinear, bicubic, etc. A good compromise between speed and accuracy that is used in the literature is generally bilinear interpolation [16], except in the specific case described in Section 3.1.4.

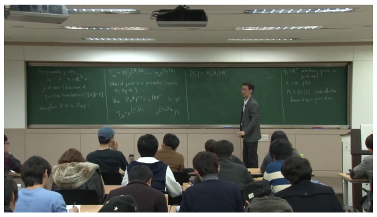

(a) Original image, 1280×720 pixels

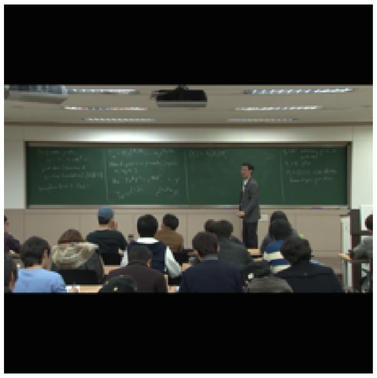
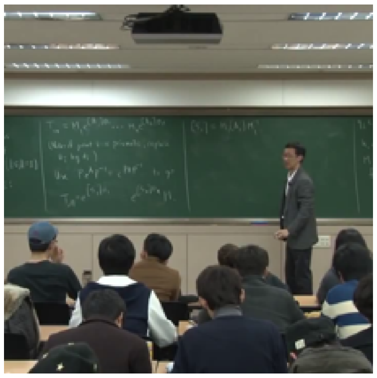
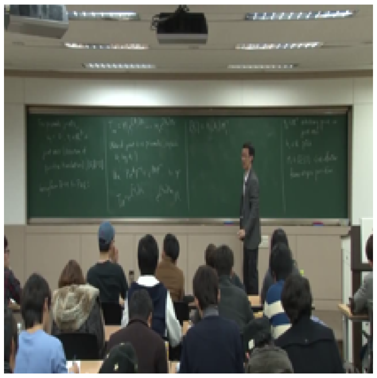

(b) Fill, 227×227 pixels (c) Crop, 227×227 pixels (d) Warp, 227×227 pixels

Figure 3-3: Difference between cropping, filling, and warping in the image pre-processing step. Filling and cropping preserves in-image ratios, but objects appear smaller.

Network activations are calculated using one of four networks, depending on the task. These are the standard AlexNet distributed with Caffe [21], PlacesCNN [49], HybridPlacesCNN [49], and a custom network fine-tuned from Places (described in Section 4.1.4). The feature extractor does a forward-pass of each frame, saving the activations from all layers of the network. All these features are passed to the feature processor. A choice in model selection is which network features to use. PlacesCNN is tuned with scenes rather than objects, so we expect PlacesCNN to perform better than AlexNet or HybridplacesCNN when looking for bounding box estimations, according to recent work in object detection from scene prediction [48]. So in the model selection stage, multiple networks are tried and the best one is used in practice.

3.1.3 Feature processor

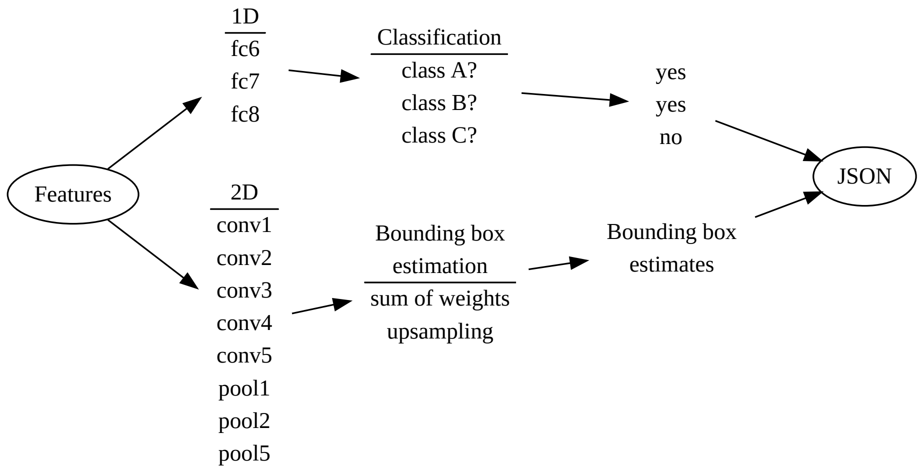

Figure 3-4: System diagram for feature processor

The extracted features from a network forward-pass are either one-dimensional or two-dimensional. From the architecture of AlexNet described in Figure 2.1 and Table 2.1, passing an image through the network in a forward pass results in over 10000 unit activations (and over 750000 individual activations) in 11 different layers of the network. Two kinds of features emerge: (1) one-dimensional feature vectors, such as fc6, fc7, and fc8, which are numerical image descriptors of the entire image, and (2) 2-dimensional units, such as a single set of activations for a specific convolutional or pooling layer output. The one-dimensional feature vectors are used for classification, and the two-dimensional units are used for bounding box estimation. See Figure 3-4 for a summary of the feature processor.

Classification, or feature processing from 1D feature vectors

The one-dimensional feature vectors are input into a trained SVM classifier that can classify an entire image into a particular scene category. SVMs are used for ease of use and training. In model selection, 10-fold cross-validation accuracy was used to determine the best features and SVM parameters to use. The accuracy of the video production style classifier is discussed in Section 4.1.3.

Mask generation from 2D units

The 2D units are used to generate a rectangular bounding box estimate from an image. Each unit can be a mask over the entire image, based on the values in the unit activations. Figure 3-5 shows an example of an image and the masks that are generated through various operations on a specific unit. To generate a mask P from one unit, the unit is preprocessed in the opposite way that the image was preprocessed before going into the network. In the simplest case, if the image was warped before being passed through the network, the unit is upsampled and rescaled to the size of the original image. If the image was initially filled then scaled, then the activation must be scaled then un-filled (in other words, cropped). Because the goal is to estimate a rectangular bounding box, nearest-neighbor estimation is used. In addition to inverse preprocessing, the unit is thresholded, either before or after the upsampling. The thresholding operation can be intuitively thought of as a filtering operation - while the unit activations may contain all the true positive activations, they will have small false positive activations that are amplified during the upsampling process, and thresholding filters out potential false positives. The EdVidParse pipeline thresholds after upsampling to avoid nonlinear optimization during training. A 2D unit is used to generate an image mask that can then be used for bounding box estimation.

For example, Figure 3-5 shows an image containing a person, and the activations

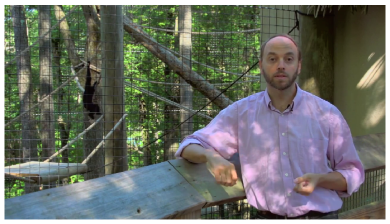

(a) Original image

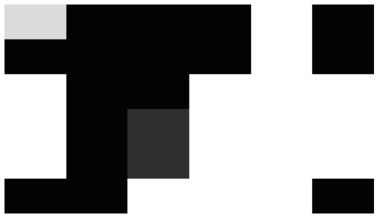

(b) Nearest neighbor interpolation, no thresholding

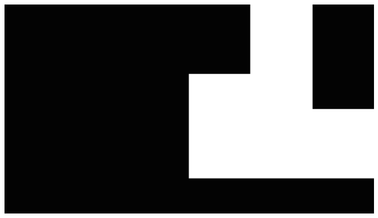

(c) Thresholding, then nearest neighbor interpolation

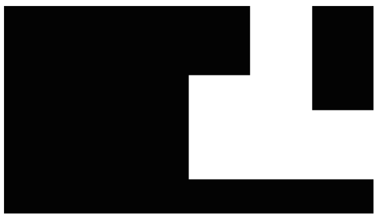

(d) Nearest neighbor interpolation, then thresholding

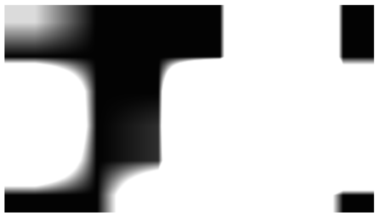

(e) Bilinear interpolation, no thresholding

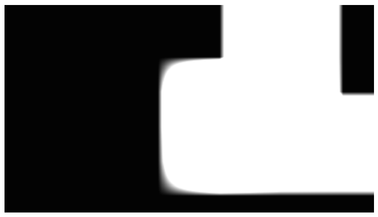

(f) Thresholding, then bilinear interpolation

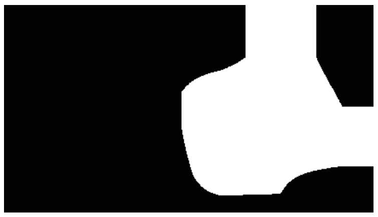

(g) Bilinear interpolation, then thresholding

Figure 3-5: A single unit serves as a mask on the original image. If the unit is trained to recognize specific objects, the mask can give hints about where the object is located. An image and the interpolated activations from unit number 138 in the pool5 layer of the Places network is shown.

of a particular unit in conv5 known to have high activations for faces. The activations are shown with a few options for interpolation and thresholding. Nearest neighbor interpolation and thresholding are commutative operations, whereas bilinear interpolation and thresholding are not.

Generating masks from the same unit activations over many images, it is compelling that specific units activate to specific objects [48]. For example, as shown in Figure 3-6, looking at the activations from unit 3 in the pool5 layer, it is clear that this particular unit responds well to faces. More unit visualizations are shown in Appendix A.

The examples shown in Figures 3-5 and 3-6 are masks generated from a single unit, but multiple units can be used for more accurate estimation. Single-unit acti-

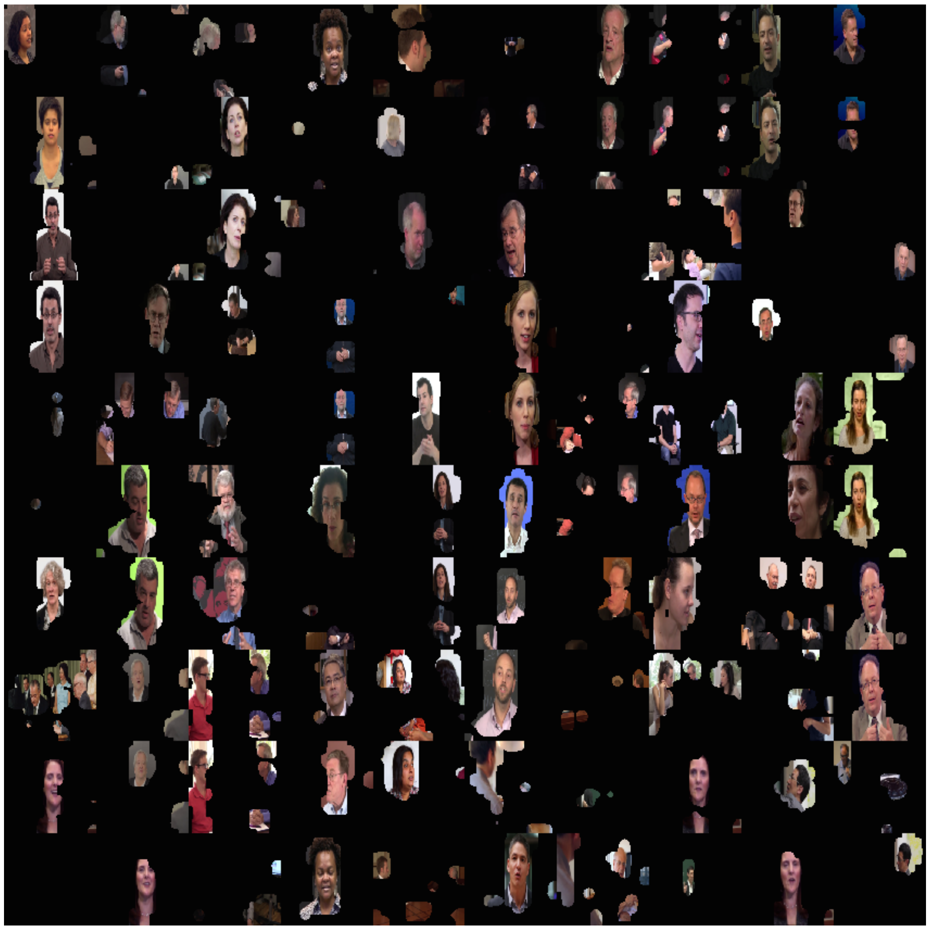

Figure 3-6: Activations from unit number 3 from the conv5 layer using the Places network over 100 images in the educational video dataset.

vations, most often from pool5, have been studied as features to use out-of-the-box for classification or regression tasks, as discussed in Section 2.3.2. However, we claim that using a linear combination of unit activations will achieve better domain adaptation for object classes not in the original network training set, as in the case of educational videos. In other words, a prediction mask P is calculated from a subset of unit activations by

$$P = WF = \sum_{f \in \text{ units}} (w_f f), \quad \text{sparse } W \tag{3.1}$$

where f is a single 2D unit activation and w_f is a scaling weight for all activations in that unit. The weights are learned for each specific object class, as described in Section 4.2. Sparse weights are desired because it reduces overfitting of the units in addition to reducing computation. The mask P is fed into the bounding box estimator.

EdVidParse uses a single threshold on P rather than thresholding each individual unit f. An extension of this project using non-linear optimization techniques to learn individual unit thresholds can potentially produce better results.

Bounding box estimation from an activation mask

An activation mask is turned into a bounding box estimate for an object with a series of thresholding and estimation operations.

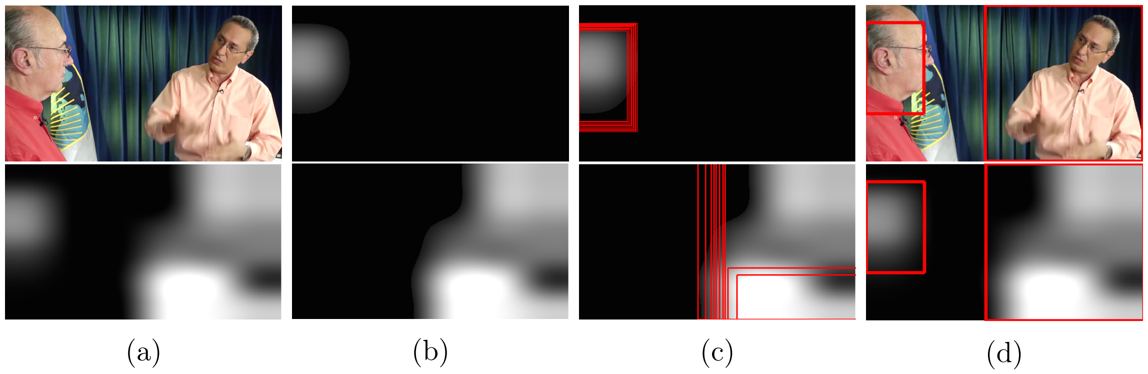

Figure 3-7: Turning an activation mask P into a bounding box. (a) The original image is turned into a thresholded activation mask. (b) The mask is split into connected components. (c) Multiple boxes are generated from each connected component. (d) Non-maximal suppression is applied to find only the best boxes.

After calculating an activation mask P for a particular object class, P is thresholded and split into connected components. For each connected component, a number of bounding boxes are generated and a score is calculated for each box around the activations of that connected component. Then, on the boxes generated for the entire image, non-maximal suppression is performed to give an optimal set of bounding boxes for the object in question. An example of taking an activation mask and turning it into a bounding box is shown in Figure 3-7. The threshold parameters are learned based on the detection task, such as the person and content detection task described in Section 4.2. To find the optimal noise-removal threshold, the mask P is subject to multiple thresholds, and connected components are calculated for each threshold.

The score S for each box is the ratio between the average activation in the box and the average activation in the image, shown in Equation 3.2. Non-maximal suppression is then performed on all boxes at all thresholds with scores S.

$$S = \frac{\sum\limits_{a \in \text{box}} a}{\sum\limits_{a \in \text{image}} a} \cdot \frac{\text{area of image}}{\text{area of box}} \tag{3.2}$$

The highest-scoring bounding boxes above a score threshold are the bounding box estimates for that object class.

3.1.4 Training and evaluating the bounding box estimator

The bounding box estimator does simultaneous detection and classification of a given object class. The idea is to train the estimator with a small number of bounding-box-annotated images of a particular class and rely on the internal network representation of the image to generate the bounding box.

A training set annotated with ground-truth bounding boxes for people and content is converted into binary masks of size 55×55 (because this is the size of the largest unit from conv1). An image without a positive example of the class is all black. These binary ideal activation masks flattened into a matrix are the ground truth activations G. In an ideal world, they are the activations we would like to generate through a linear combination of unit activations, which would map exactly to the bounding boxes we want to generate. Because of the ReLU units used in each neural network layer, the unit activations will have only positive values, meaning that an image without a positive example will be returned all black from the network, mirroring our training data.

All the training images are then passed through the network, and all the internal unit activations are resized to 55×55 using nearest-neighbor interpolation to create the unit matrix F.

We then learn a set of weights W to minimize the pixel-level L2 error E over all images in the training set, shown in Equation 3.3. We want to L1-regularize the W

matrix to rely on a sparse set of units F.

$$E = \sum_{\text{images}} \sum_{\text{pixels}} (G - WF)^2 \tag{3.3}$$

However, there is a practical limitation to computing this matrix W in its entirety. With a training set of merely 50 images, all the activations in the 2D units scaled to equal size of 55×55 to construct the F matrix will take approximately 2.5 GB to store in memory, assuming a float takes 8 bytes of memory.[1] This poses a problem for finding an exact sparse solution of unit weights W, because the least-squares solution requires computing $F^T F$, or having two copies of F in memory simultaneously.

Instead, we propose a greedy algorithm that takes advantage of the simultaneous optimizations we would like to do. First, iterate through all the units, solving the least squares problem in Equation 3.3 with each unit one by one to find the unit that yields minimum error. Then, for as many units as desired, iterate through the units to solve the least squares solution for the growing list of best-fit units. The advantage of this algorithm for finding optimal units is that it iteratively builds the units that best complement one another. If a particular unit is chosen because it provides the smallest error when it stands alone, the next maps are chosen specifically based on the performance of the first. No assumptions are made about the weights - they do not have to be positive. Negative weights imply that the activations of a particular unit provide a negative estimate about the presence of the particular object class. In practice, all the weights that are computed by this method are positive, implying that the algorithm learns to construct positive activations rather than deconstruct negative activations.

Once the weights W are learned, the bounding box is estimated as described in Section 3.1.3. Model selection is performed on how many units to use, which features to use to extract the unit activations, and the final thresholding operation. A bounding box can be extracted with weights and a threshold learned from this method in under one second on a CPU, since only a single forward-pass through the

[1] 8 bytes $\times 772544$ filters $\times (55 \times 55)$ activations per filter $\times 50$ images ≈ 2.5 GB

network is required.

One potential limitation to this greedy approach is that it is possible to find a set of units that work better together than separately. For example, the first unit found by the algorithm minimizes the pixel-level error, but it is possible that the two units that would minimize the pixel-level error do not contain the first found unit. To combat this and provide regularization with our training data, once the final units are found, we train the weights using L1 regularization to ensure sparsity. It is not guaranteed that a single unit will work for bounding box estimation, and in practice the best performance occurs with 2 or 3 units.

3.1.5 Potential improvements

One limitation of the algorithm in its current state is that the algorithm does not take into account the "random noise" responses of its activations. A given unit responds with high activation to the image region that contains the object of interest, but it also responds to other parts of the image with some small activations that can effectively be considered noise. To account for this, we choose to learn a single threshold at the end of the linear combination to filter out this activation noise. However, in practice this is not as effective as thresholding a single set of unit activations before the weights are learned. If a set of thresholds and weights is learned simultaneously for the units, the problem becomes a non-linear optimization problem that is hard or impossible to solve by analytical means. Early experiments with learning unit weights yielded thresholds that were close to zero, so this work lays does not attempt to learn a set of thresholds for each unit. More experiments are needed to determine whether this non-linear optimization will prove more effective than the results given here.

An additional step that might offer improvement is learning a bounding box regression algorithm that takes as input the bounding box from the estimator and regressing to a bounding box that is potentially more correct, like the approach taken by Girshick et. al. [16].

3.2 Advantage over R-CNN

There are a number of downsides to using R-CNN, the existing method for object detection using deep features [16], and EdVidParse improves on these disadvantages. The effectiveness of R-CNN strongly depends on the image preprocessing step, there are many parameters to tune, the method is very slow at train and test times, and there no information about the internal image representation is used in prediction. However, an advantage is that R-CNN can be very accurate. EdVidParse is invariant to preprocessing, has few parameters, is fast to train and test, and uses internal network representations for prediction.

The R-CNN pipeline involves generating object proposals for a given image (typically 1000 or more), preprocessing that image region, extracting fc7 features from the network, and classifying the image region with an SVM for each object class. During training, thousands of object proposals are generated, sent through a network, and used to train the SVM with hard negative mining. In contract, EdVidParse takes unit activations from a single forward-pass in the network and constructs a bounding box from the unit activations.

In R-CNN, the choice of image preprocessing greatly affects the outcome of the classification. If a proposed image crop is highly non-square, simply warping the crop will produce an image that is also hard for humans to identify. In the example of detecting people and content in educational videos, this is especially a problem, as shown in Figure 3-8. The fc7 features extracted from these image patches will be different enough that a classifier trained on these images will not be invariant to all kinds of preprocessing. EdVidParse on the other hand, because it depends on internal network representations, is invariant to image pre-processing.

Additionally, in R-CNN training there are many parameters to tune - each set of SVM parameters in addition to the object proposal algorithm parameters (of which there can be 10s of parameters), the hard negative mining parameters, and others. Training R-CNN end-to-end with Bayesian optimization is not an option, since training the entire system takes too long and Bayesian optimization shows limited

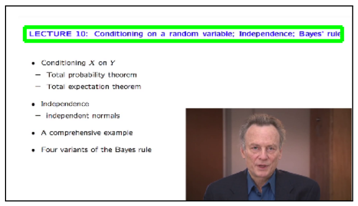

LECTURE 10: Conditioning on a random variable; Independence; Bayes' rule

- Conditioning X on Y
  - Total probability theorem
  - Total expectation theorem
- Independence
  - independent normals
- A comprehensive example
- Four variants of the Bayes rule

(a) The original image and bounding box

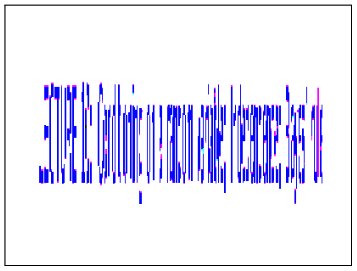

(b) Extracted and warped

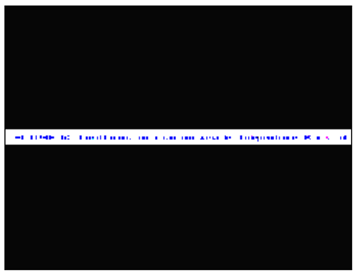

(c) Extracted and filled

Figure 3-8: An example of an image region that, when sent through the R-CNN with simple warping, will not yield good results. In this case, cropping and filling will yield similar results because the bounding box is highly rectangular.

improvement over grid search for large sets of parameters. In our comparison experiments between our proposed algorithm and R-CNNs we train each piece of the R-CNN pipeline separately, like the original authors. By contrast, EdVidParse has a small number of parameters that can be trained end-to-end.

Finding object detections in a single video frame for R-CNN is very slow. With 1000 or more object proposals to generate for each frame, each one has to be resized and interpolated for network processing, passed through the network, then ranked and sorted to perform non-maximal suppression. This results in around 1000 forward-passes through the network, one for each object proposal. In EdVidParse, only a single forward-pass is needed, decreasing the processing time by a factor of 100 or more.

R-CNNs do not take advantage of any of the internal network representations of the images in the network. It only relies on fc7 features, which do not have any physical meaning for the image, discarding any unit activations from lower in the network. In contrast, EdVidParse takes advantage of the internal network representations and does not discard information.

However, a distinct advantage of R-CNNs is the ability to train the final SVM with hard negative mining, with as many examples as needed to get the desired performance. With the almost exhaustive list of object proposals, the AP score achieved with R-CNNs can be as high as 0.90 depending on the training set. When high accuracy is desired and speed is not an issue, R-CNNs prove a valuable tool for object detection. Because one of the design goals of EdVidParse was speed, using internal feature representations was much faster than using R-CNN.

3.2.1 Using object proposals for bounding box estimation

EdVidParse generates bounding boxes around objects, but does not benefit from using an object proposal algorithm before bounding box estimation. The edge boxes object proposal algorithm used in R-CNNs is extremely fast and highly tunable [50]. For a given set of training images annotated with object bounding boxes, the parameters are tunable to achieve high recall for that object class.

The object proposal algorithm used in comparisons of R-CNN and EdVidParse is the edge boxes algorithm described by Zitnick, et. al. [7, 8, 50]. The basic idea of the edge box algorithm is that objects in an image have certain edge properties. For example, an object generally has a large cluster of complete edges inside a square region. According to some tunable parameters, such as how far apart to sample boxes across the image, the edge boxes algorithm can be tuned for images of particular sizes or images that have particular objects. An example of using object proposals with EdVidParse is described in Section 4.3 about reconfiguring picture-in-picture images.

To combine object proposals and bounding box estimation, generate a set of object proposals and assign each box a score according to the formula given in Equation 3.1. This can solve the problem of how to generate bounding boxes from the unit activations as described in Section 3.1.3. However, the downside to this approach is that the bounding boxes that get generated in the final image are then limited to the bounding boxes proposed by the edge boxes method. Zitnick et. al. claim that on the PASCAL dataset, 96 percent recall is achieved with an acceptable overlap tolerance of 0.5, and 75 percent with the stricter overlap tolerance of 0.7 [50]. This means that the success of the overall bounding box estimator is dependent on the object proposal estimator, since the recall is not 100 percent.

In our experiments, we achieved worse recall rates for classes that did not originally appear in the PASCAL training set, namely for text content. Using object proposals and assigning scores to them using the bounding box estimator method yielded worse results across all classes compared to not using them, and this is probably because the success of the final estimation is limited by the object proposals and therefore by that algorithm. However, Section 4.3 gives an example of a use case where, because of strong priors on the kinds of boxes we want to generate, using edge boxes can guarantee increased performance.

Chapter 4

Applications

This section will describe three case studies for using EdVidParse to do three tasks related to educational videos: (1) classifying videos by production style, (2) generating bounding box predictions for people and content, and (3) reconfiguring a picture-in-picture video.

4.1 Classifying video production style

4.1.1 Problem

Videos in online courses come in many different styles, and EdVidParse can answer questions related to video style. For example, some videos are filmed in a production studio with an instructor lecturing at a podium, and others are classroom lecture recordings cut into pieces and posted online. Sometimes an instructor's face features prominently, other times the video is a presentation with a voiceover. Some videos even vary style mid-video, for example from classroom recording to a close-up of a slide. Researchers are interested in questions like whether high production value videos or the presence of a lecturer in a frame increased student engagement.

In the study by Guo et. al. [18], the question is the correlation between video production style and student engagement. For this study, researchers used a number of videos from four computer science courses on edX, and gave each video a single production label. The conclusions from the study were that high production cost videos do not increase student engagement. However, EdVidParse can offer greater insight into this question, since it can classify videos into categories on a more granular level, giving a label to each frame.

EdVidParse classifies each frame in an educational video into one or none of 9 labels described in Table 4.1 using an SVM classifier on top of fc7 features with a test set accuracy of 86 percent. To accomplish this task, a hand-labeled dataset was used for training and testing.

4.1.2 An educational video dataset

Data collection

A set of educational videos was collected and annotated for training and testing. Educational videos are available free of charge from edX for registered course users. To take advantage of this, an automated script using Selenium [3] auto-registered for all of the courses offered on edX in September 2014 and scraped the pages for all links to videos hosted on YouTube. A total of 6914 video URLs were collected from 181 courses from varied disciplines.

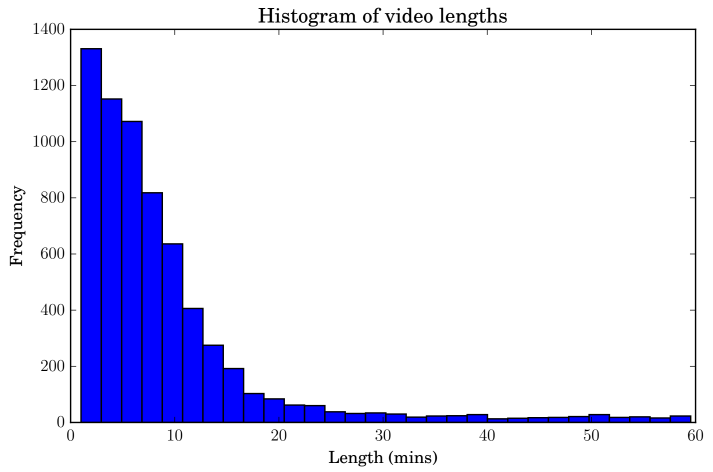

Figure 4-1: Histogram of video lengths from the scraped edX videos

Because all the edX videos are hosted on YouTube, basic information about the videos, such as length and frame rate, can be accessed via the YouTube API. Figure

4-1 shows the distribution of video lengths of the videos scraped from edX, where the average video length was 9.11 minutes, consistent with the findings from Guo's study. Nearly all videos had a frame rate of 30 frames per second (fps), so they were very high quality.

To create a dataset, 1600 frames were randomly selected. First, 800 URLs were randomly selected from the scraped list. Then, from each video, two random times were selected. Each frame was labeled with both a scene label and with object annotations. Any frame that was all black or that was a fading transition between two types of frames was rejected from the dataset. In total, 1401 images were split into a training set and testing set. The test set has 20 images from each class label, and the rest of the images make up the training set.

Scene annotations

Scene annotations are assigned labels from a semantic understanding of the world. Humans are able to identify a dining room, despite there not being a standard dining room template. While there are visual similarities between scene types, there are even more differences. This idea can be applied to frames from educational videos, giving each extracted frame a single label describing the type of scene in the frame.

The scene labels used for this dataset were a modified list taken from Guo's study. A full list of scene labels together with a description is shown in Table 4.1. The *office* label assigned by Guo was renamed *head* to make it more general. To accommodate various styles of videos and single them out specifically, more categories were added, such as *picture-in-picture* (abbreviated to *pip*), *synthetic*, and *discussion*, that were not specifically mentioned by Guo because those types of videos were not common in computer science courses that were the focus of the study. Examples of each kind of scene label are shown in 4-2, and a frequency histogram for each label is shown in Figure 4-3. Because of the imbalance in class frequencies, the test set contains 20 examples of each class label, so test set accuracy and the confusion matrix are reported for accuracy. When some categories had limited data, videos were found manually for more examples to ensure at least 50 examples per class.

Scene labels	Description
code	A software demo or full-screen code-writing in an IDE
discussion	Multiple people in a frame talking
Khan-style	Free drawing on a tablet or paper, in the style of videos popularized by Khan Academy
talking head	Mostly contains the instructor
lecture	From a live classroom recording
picture-in-picture	Slide with a square overlay of an instructor in a corner
slide	PowerPoint-like slide presentation, just with educational content, sometimes containing just images
studio	Staged recording of an instructor in a studio with no audience
synthetic	An instructor and an overlay of slide content, but not in rigid format like *picture-in-picture*

Table 4.1: Scene label categorization description

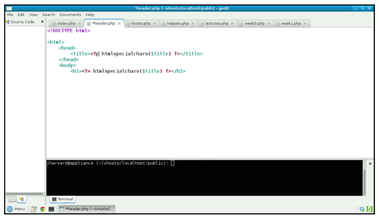
*header.php (~/vhosts/localhost/public) - gedit
File Edit View Search Documents Help
Source Code
index.php *header.php footer.php helpers.php lectures.php week0.php week1.php
Terminal

```
<!DOCTYPE html>

<html>
    <head>
        <title><?p htmlspecialchars($title) ?></title>
    </head>
    <body>
        <h1><?= htmlspecialchars($title) ?></h1>
```

```
jharvard@appliance (~/vhosts/localhost/public):
```

(a) *code*

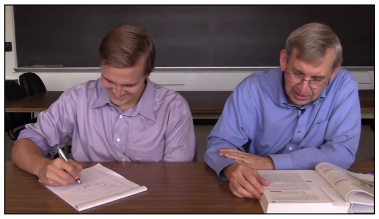

(b) *discussion*

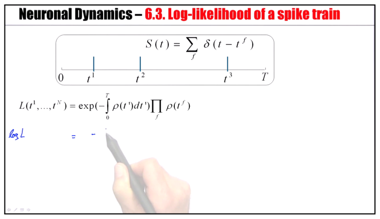

$S(t) = \sum_f \delta(t - t^f)$

$L(t^1, \ldots, t^N) = \exp(-\int_0^T \rho(t')dt') \prod_f \rho(t^f)$

(c) *Khan-style*

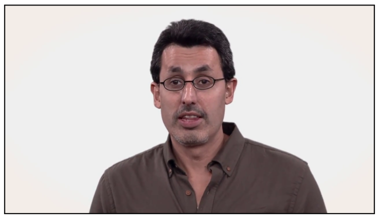

(d) *talking head*

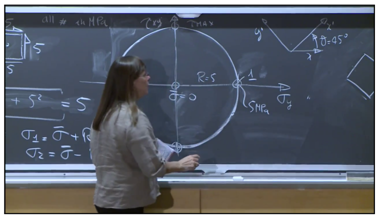

(e) *lecture*

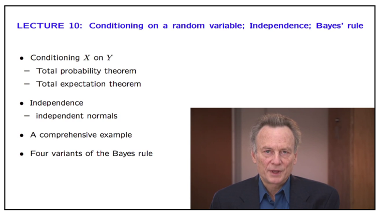

LECTURE 10: Conditioning on a random variable; Independence; Bayes' rule

- Conditioning X on Y
  - Total probability theorem
  - Total expectation theorem
- Independence
  - independent normals
- A comprehensive example
- Four variants of the Bayes rule

(f) *picture-in-picture*

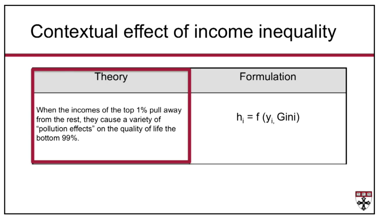

Contextual effect of income inequality

Theory	Formulation
When the incomes of the top 1% pull away from the rest, they cause a variety of "pollution effects" on the quality of life the bottom 99%.	$h_i = f(y_i, \text{Gini})$

(g) *slide*

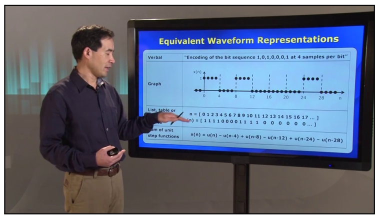

Equivalent Waveform Representations

Verbal	"Encoding of the bit sequence 1,0,1,0,0,0,1 at 4 samples per bit"
Graph	
List, table or	n = [0 1 2 3 4 5 6 7 8 9 10 11 12 13 14 15 16 17 ...] n) = [1 1 1 1 0 0 0 0 1 1 1 1 0 0 0 0 0 0 ...]
m of unit step functions	x(n) = u(n) – u(n-4) + u(n-8) – u(n-12) + u(n-24) – u(n-28)

(h) *studio*

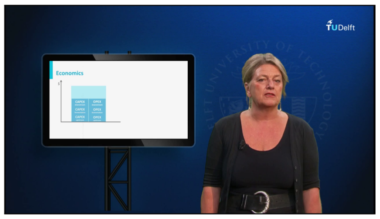

(i) *synthetic*

Figure 4-2: Example frames for scene labels

Labels were chosen in an attempt to minimize ambiguity using their original semantic definitions. For example, a frame that contained a full-frame picture of a famous person was classified as *slide* rather than *head* since it represented slide content presented to a leader, and slides that a person drew on to progressively explain

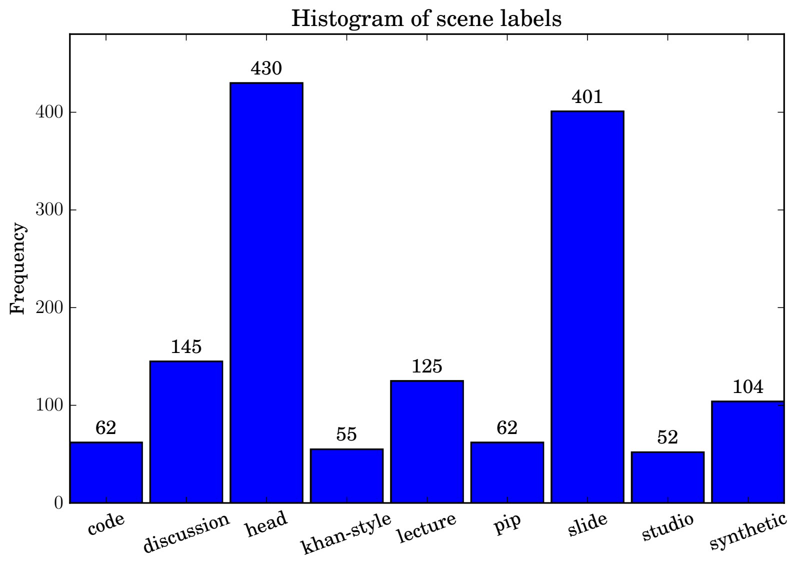

Figure 4-3: Frequency histograms for scene labels in the educational video dataset

concepts was labeled as *Khan-style*.

4.1.3 Results

The overall test set accuracy is 86 percent classification accuracy. Each class SVM is trained separately, then used together for test classification. Table 4.2 gives the confusion matrix for the classifier, showing that the classifier more likely doesn't classify an object into a category rather than confusing two categories.

Each class is trained with a separate linear kernel SVM. The best model for each class was chosen based on which combination of fc7 features (AlexNet, Hybrid-placesCNN, PlacesCNN) and SVM parameters (L1 / L2 regularization, C value, bias) had the highest 10-fold cross-validation accuracy on the combined training and validation sets. All images were warped for classification, because this is how the networks were trained. Gaussian kernel SVMs are not used in training to avoid overfitting. A Gaussian kernel exploits nonlinear relationships between the data points and can find separating planes between the data when there are none, so to avoid overfitting on the limited training data, Gaussian kernels were not used.

At test time, an image from the test set is classified with all 9 SVMs and assigned

		Predicted label									
		code	*discussion*	*head*	*khan-style*	*lecture*	*pip*	*slide*	*studio*	*synthetic*	*other*
True label	*code*	0.75									0.25
	discussion		0.95								0.05
	head			0.95							0.05
	khan-style				0.75						0.25
	lecture					0.85					0.15
	pip						0.75				0.25
	slide							0.95			0.05
	studio								0.85		0.15
	synthetic									0.95	0.05

Table 4.2: Confusion matrix for video production style classification

one class label based on which decision value is greatest. For example, an image can get an SVM score of 0.95 from label 1 and 1.35 from label 2, so even though the image was given a positive score by two models, it will be assigned label 2 because the decision value is greater. An image with no positive classifications is not given a label, so it is classified as *other*.

4.1.4 Discussion

The overall test set accuracy is 86 percent on the held-out test set, and the confusion matrix is given in Table 4.2. EdVidParse is more likely to not classify a label at all than confuse that label with another class. The classes that are hardest for EdVidParse to classify are the *code*, *Khan-style*, and *picture-in-picture* classes, which do not get classified correctly 25 percent of the time. Overall the classifier performs well when presented with many different kinds of images, especially on the *discussion* and *head* labels, since they are very distinct visual categories.

Despite the visual similarity between *code* and *slide* frames, the classifier can distinguish between the two types well, more likely not assigning a label at all rather than incorrectly classifying the frame. There are no classes that are commonly confused by the classifier, and the most common failure more in general is that a given frame is not classified into any category rather than being incorrectly classified.

A limitation of this multiclass SVM approach is that the class labels were unbalanced for training. While the test set was kept constant at 20 examples per class, some classes had more training examples. This meant that for a class like *head* that had many training examples, the classifier makes few mistakes. However, for a label like *Khan-style*, there are few examples, so more frames are not correctly classified as *Khan-style*.

Another limitation with this classification scheme (as compared with the study from Guo, et. al.) is that it classifies individual video frames, whereas some of the video production styles may be easier to distinguish when a few adjacent video frames are taken together. For example, the difference between a *Khan-style* frame and a *slide* is more noticeable when notes are seen written on the screen in adjacent frames. However, this approach is future work that is not covered by the scope of this project. The classification accuracy can be improved by using hard negative mining with image crops from the frames that do not have a particular image label.

Different network features performed best depending on the type of semantic label. AlexNet features perform the best to identify slides, perhaps because they are visually similar to signs, which is an object label used in the original AlexNet training set. Places features perform better for labels that rely on seeing the entire image to classify the scene, such as *picture-in-picture* and *lecture*, because those are more easily decomposed into constituent scene parts. The HybridplacesCNN network was trained with both object data and scene data, so frame types like *code* perform best with Hybridplaces features, since there is both object elements like text and scene elements like the frame around an computer window.

The end-result classifications for video frames are extremely fast to calculate - a forward-pass through the network for each frame on a CPU is under 1 second, and the SVM classification is a single matrix multiplication.

Using these scene annotations, the PlacesCNN network was used as a baseline for finetuning a network to directly classify frames into one of the 10 proposed classes. The hand-labeled set was used as a test set, and another random 10000 images were classified using the trained SVM classifiers reported above. This is an approach of semi-supervised learning, where many frames are classified with weak supervision (using the roughly-calculated SVM classifiers trained on supervised data) are used for training, and the supervised smaller dataset is used for testing. According to the fine-tuning procedure recommended by the creators of Caffe, the learning rate was increased in the fully-connected layers and the overall learning rate was decreased from the PlacesCNN learning rate. In the end, because the amount of data used for fine-tuning was small, the network achieved 90 percent accuracy on the test set, most likely due to overfitting. However, in subsequent tests for bounding box estimation, the fine-tuned network did not perform better than PlacesCNN or HybridplacesCNN, perhaps because the changes in the convolutional layers did not happen appreciably from the fine-tuning.

4.2 Extracting people and content for VideoDoc

4.2.1 Problem

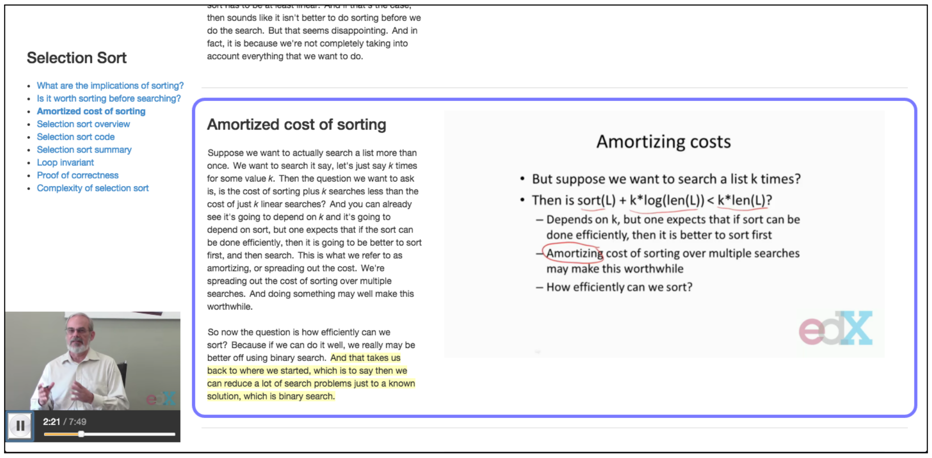

then sounds like it isn't better to do sorting before we do the search. But that seems disappointing. And in fact, it is because we're not completely taking into account everything that we want to do.

Selection Sort

- What are the implications of sorting?
- Is it worth sorting before searching?
- **Amortized cost of sorting**
- Selection sort overview
- Selection sort code
- Selection sort summary
- Loop invariant
- Proof of correctness
- Complexity of selection sort

Amortized cost of sorting

Suppose we want to actually search a list more than once. We want to search it say, let's just say *k* times for some value *k*. Then the question we want to ask is, is the cost of sorting plus *k* searches less than the cost of just *k* linear searches? And you can already see it's going to depend on *k* and it's going to depend on sort, but one expects that if the sort can be done efficiently, then it is going to be better to sort first, and then search. This is what we refer to as amortizing, or spreading out the cost. We're spreading out the cost of sorting over multiple searches. And doing something may well make this worthwhile.

So now the question is how efficiently can we sort? Because if we can do it well, we really may be better off using binary search. And that takes us back to where we started, which is to say then we can reduce a lot of search problems just to a known solution, which is binary search.

Amortizing costs

- But suppose we want to search a list k times?
- Then is sort(L) + k*log(len(L)) < k*len(L)?
  - Depends on k, but one expects that if sort can be done efficiently, then it is better to sort first
  - Amortizing cost of sorting over multiple searches may make this worthwhile
  - How efficiently can we sort?

Figure 4-4: Screenshot of the VideoDoc interface, which combines textual and video information into one interface

A second application of EdVidParse is estimating bounding boxes for people and textual content in video frames. In an attempt to explore the way students can interact with static videos, a project called VideoDoc combines video information with transcripts to subdivide the video into digestable sections, including separating a talking head from progressing slides of notes [28]. Figure 4-4 shows a screenshot of the VideoDoc interface. The main idea is to break up a video into smaller sections, dictated by either a change in video viewpoint (such as a transition between a talking head and a slide) or by a slide change.

EdVidParse provides a first-pass input to the VideoDoc system, taking a video and outputting bounding box estimates in each frame of people and textual content, the two salient objects used by VideoDoc. The person and content extractor uses all the internal network features from the feature extraction stage and the bounding box estimator described in Section 3.1.3. EdVidParse cannot distinguish between slides, but can provide an estimate for viewpoint transitions within the video. A VideoDoc creator can then clean up the annotations manually for the ones that were incorrectly identified.

VideoDoc poses a number of object detection challenges for EdVidParse: How can pictures of famous people in slides be marked as content rather than people? Can internal network features discriminate between numbers of people in a frame?

4.2.2 Object annotation dataset

Each frame from the scene dataset described in Section 4.1.2 was annotated with bounding box locations of all the people and the content in the frame. Content is defined as textual content meant for a student to take notes on, such as graphs, formulas, text, diagrams, code, etc. When the entire frame contains a slide, a tight bounding box is drawn around the content rather than marking the entire frame. As much of a person or his body that is in the frame is labeled as a person. Because people and content are broad semantic categories, there are a wide range of objects that fit the labels. There is little value in identifying a full-body person versus a person's face, since the size of the bounding box can provide this label instead. In the dataset there were a total of 833 content bounding boxes and 1462 people bounding boxes. Examples of annotated content and people frames are given in Figure 4-5.

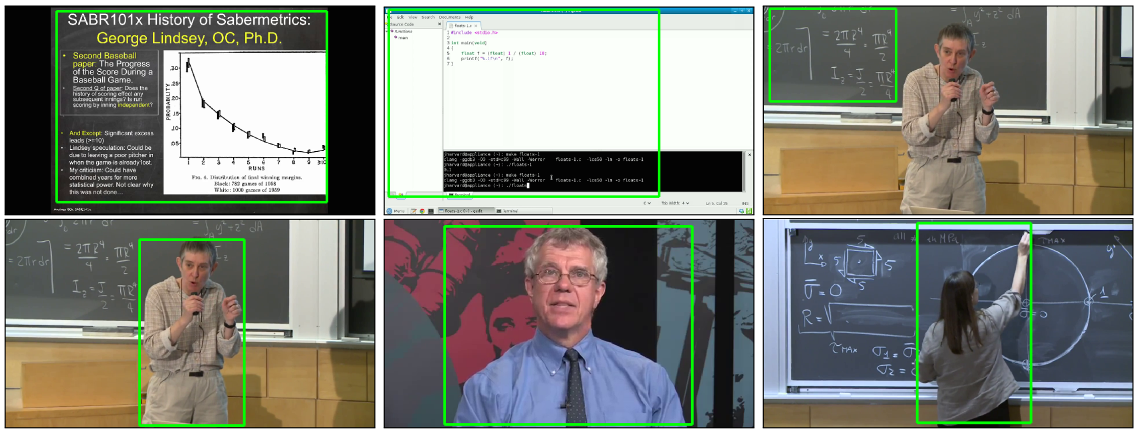

Figure 4-5: Example people and content annotations

Scene label	Best result (AP score)	Description
content	0.434	Places features, 3 units
people	0.439	Places features, 2 units
overall (mean AP score)	0.437	

Table 4.3: Object detection results

4.2.3 Results

After training, the best results for detecting people and content are described in Table 4.3, with the mean AP score for both categories at 0.437. Training was done on the training set, model selection performed on the validation set, and the results reported on the test set.

An example of correctly-detected people and content is shown in Figure 4-6. A correct detection means that the estimated bounding box overlaps the ground truth bounding box by 50 percent or more.

4.2.4 Discussion

The best AP score for content is 0.434 and for people the best score is 0.439, which performs well in most cases. However, there are some interesting failures.

EdVidParse cannot distinguish between people in a frame if they are too close together. If the people are farther apart, it is likely that one of the thresholding

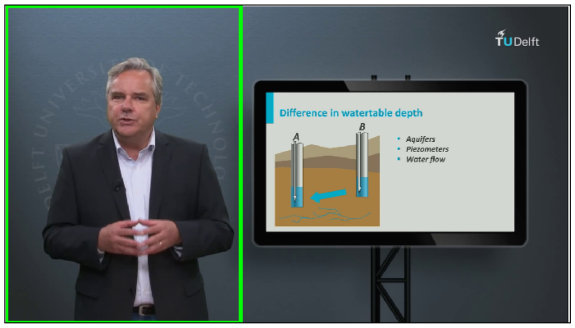

(a) A person is correctly localized.

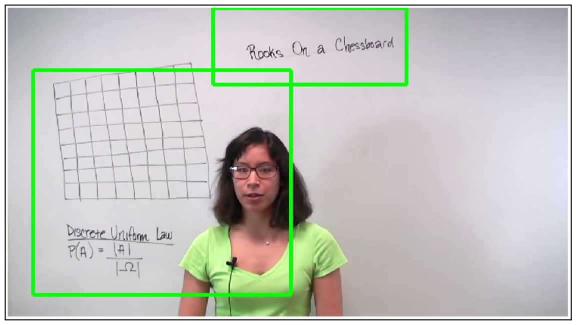

(b) Two content regions are correctly identified.

Figure 4-6: Two examples of correct person and content identifications. The green boxes are extracted boxes with a high enough score.

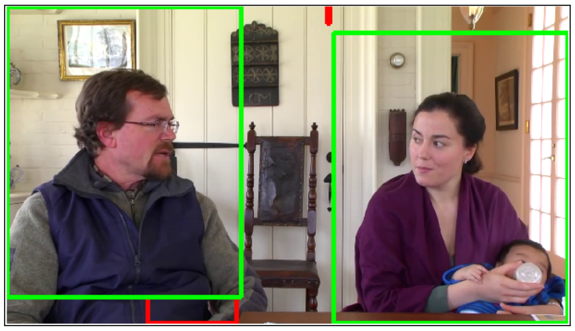

(a) The people are far enough apart that the system can distinguish them.

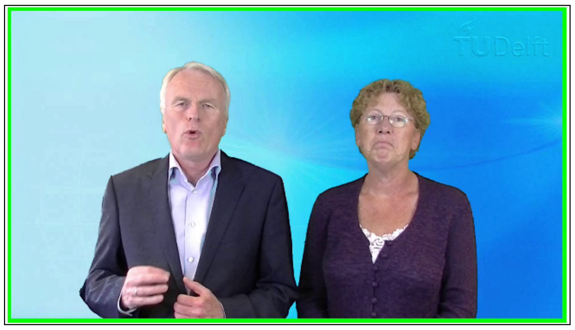

(b) The people are too close together to generate two separate boxes.

Figure 4-7: Depending on how far apart two people are, EdVidParse can generate the appropriate number of bounding boxes. Red boxes are detected boxes, and green boxes are those boxes with a high enough score to be accepted.

operations will capture two boxes, but if the people are too close together then this is not possible (see Figure 4-7). An improvement in future work is being able to distinguish between people in a frame independent of how close together they are.

Another interesting scenario is pictures or cartoons of people that appear in slides. If the photos are very life-like, the system generates bounding boxes for this person. Additionally, because the specifications for the person detector are for both faces and full bodies, when there is a lot of clutter in the frame with body parts and faces, a single large bounding box is returned. See Figures 4-8 and 4-9 for examples.

The most common feature in content areas is the presence of text, so when there are dense regions of text, the estimator correctly predicts the content regions, as

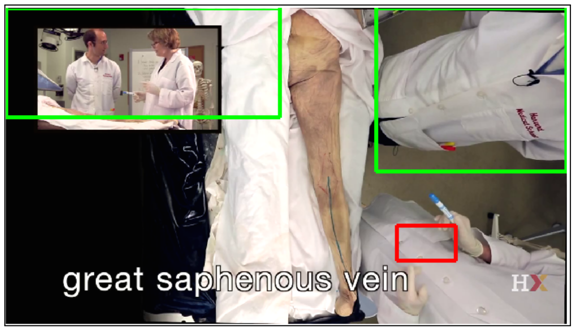

(a) Most of the frame is taken up by body parts. Some are identified, some are not.

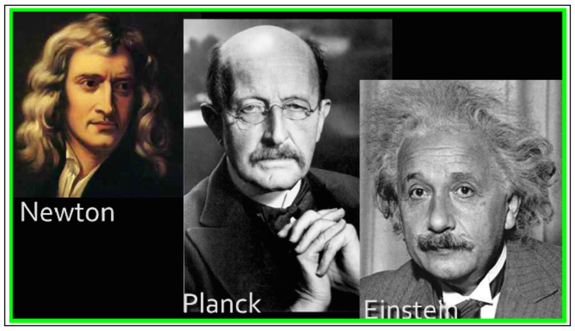

(b) These famous people look like real people, and they are too close together.

Figure 4-8: Interesting mishaps in the people estimator. Red boxes are detected boxes, and green boxes are detected boxes with a high enough score.

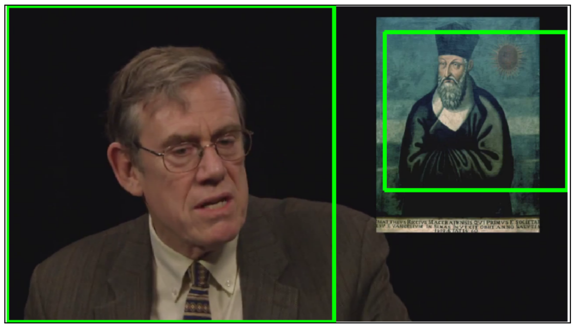

(a) The system found the real person, but also the picture of the person in the top right.

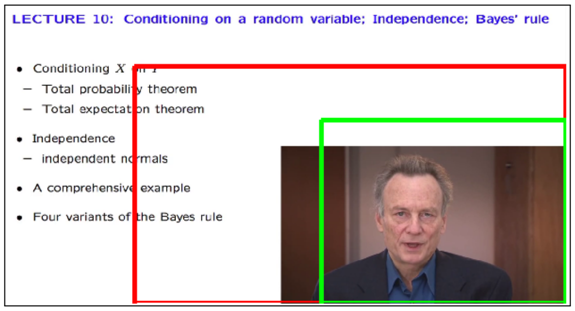

LECTURE 10: Conditioning on a random variable; Independence; Bayes' rule

- Conditioning X on Y
  - Total probability theorem
  - Total expectation theorem
- Independence
  - independent normals
- A comprehensive example
- Four variants of the Bayes rule

(b) A better score is assigned to the correct (inner) box.

Figure 4-9: Examples of successful and unsuccessful people detections by the classification system. Red boxes are detected boxes, and green boxes are the detected boxes with high score.

shown in Figure 4-10. However, for areas of long, thin text, as shown in Figure 4-11(a), the estimator does poorly. This is most likely because the activation for that area is not strong enough to withstand the thresholding stage. Also, logos often have content-like elements such as text and diagrams, so it is hard for EdVidParse to distinguish between logos and desired content, as shown in Figure 4-11(b). In fact, a failure mode for text content detection in evaluation is that, as shown in Figure 4-11(b), an area of large text might be detected as a number of different text regions, but the ground truth result might be labeled as a single box.

A number of techniques for finding the optimal filters were explored, and the kinds of units that are most useful for detecting people are different than the units

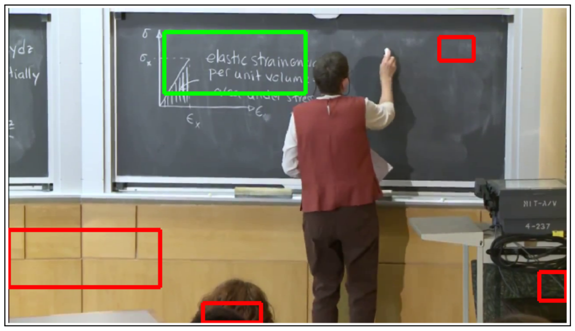

(a) One bounding box around the blackboard text.

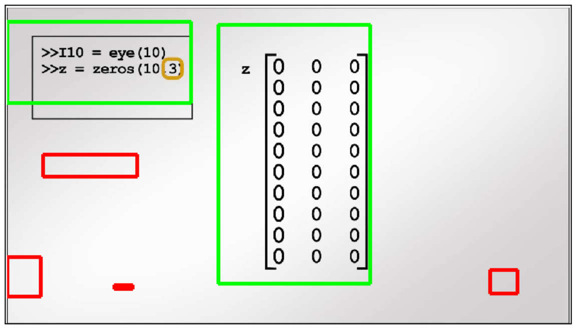

```
>>I10 = eye(10)
>>z = zeros(10,3)
```

```
z [0 0 0
   0 0 0
   0 0 0
   0 0 0
   0 0 0
   0 0 0
   0 0 0
   0 0 0
   0 0 0
   0 0 0]
```

(b) Two bounding boxes around independent regions of content.

Figure 4-10: The bounding box estimator got content exactly right, even when there were two boxes to find. Red boxes are detected boxes, and green boxes are detected boxes with a high enough score.

useful for detecting content, because they are composed of different kinds of object parts. units that are found to be predictive of people are units in pool2 and pool5 in the Places network, which suggests that people are semantic components of scenes. With content, the units come from lower down in the network, from conv4 and pool2, suggesting they are building blocks with less semantic meaning. Because people come in different configurations, we hope that the units found to activate strongly to people activate for different parts of a body - for example to a face, a leg, or a body. In practice this does not happen, perhaps because the data is not labeled with these kinds of annotations. Appendix A contains some visualizations of strongest-activating units for people and for content.

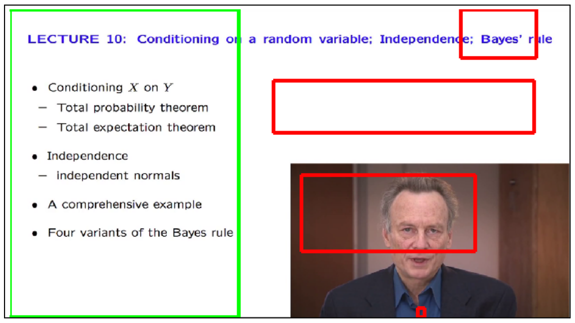

LECTURE 10: Conditioning on a random variable; Independence; Bayes' rule

- Conditioning X on Y
  - Total probability theorem
  - Total expectation theorem
- Independence
  - independent normals
- A comprehensive example
- Four variants of the Bayes rule

(a) Box-like text is easy to find, but long thin text is hard to find.

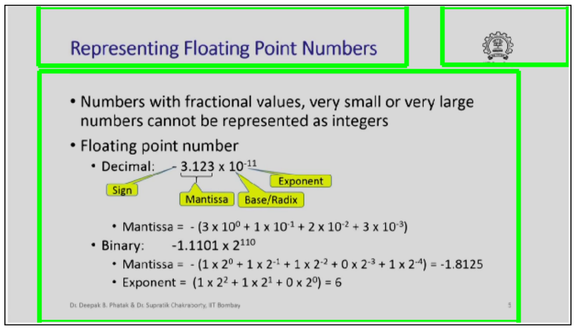

Representing Floating Point Numbers

- Numbers with fractional values, very small or very large numbers cannot be represented as integers
- Floating point number
  - Decimal: $- 3.123 \times 10^{-11}$
    - Mantissa = $-(3 \times 10^0 + 1 \times 10^{-1} + 2 \times 10^{-2} + 3 \times 10^{-3})$
  - Binary: -1.1101×2^{110}
    - Mantissa = $-(1 \times 2^0 + 1 \times 2^{-1} + 1 \times 2^{-2} + 0 \times 2^{-3} + 1 \times 2^{-4}) = -1.8125$
    - Exponent = $(1 \times 2^2 + 1 \times 2^1 + 0 \times 2^0) = 6$

(b) Logos have content-like elements, so they are also detected.

Figure 4-11: Red boxes are detected boxes, and green boxes are detected boxes with a high enough score.

4.3 Reconfiguring picture-in-picture videos

4.3.1 Problem

Educational videos are often post-processed after filming to be in the *picture-in-picture* style, shown in Figure 4-2. It has been shown that the presence of an instructor's head in the side of a frame with only text will increase student engagement. However, a student may want to view the two streams separately. For example, when a learner is reviewing slides, a talking head is distracting. But, an instructor's head is engaging when viewing a video for the first time. So being able to extract an instructor's head from a *picture-in-picture* frame can be helpful for learners.

EdVidParse can remove the smaller picture of an instructor's head from picture-in-picture videos. An added benefit of using this feature of EdVidParse is that part of the detection work is already done - the user will only want to send through a video that is already in *picture-in-picture* format, removing the need for the difficult classification step. The task is then a detection task rather than simultaneous classification and detection.

4.3.2 Results

Usually when a video is composed into *picture-in-picture* format, the inner picture is an instructor's head or body from a studio or live lecture recording. By definition the inner picture is always rectangular (if it is not rectangular then the frame is a *synthetic* frame and is not considered *picture-in-picture*). Because of this strong prior, we combine object proposals and the bounding box estimation method to provide a fast way of locating near-exact bounding boxes for the inner picture to remove.

Edge boxes rely heavily on the observation that specific objects have certain edge properties. In the case of *picture-in-picture* frames, there is a distinctive edge map because of the strong edge around the inner picture bounding box. We use these assumptions to train the edge box algorithm parameters to find the inner picture in only *picture-in-picture* frames, achieving 98 percent recall with a 0.7 overlap threshold tolerance.

But because Zitnick's object proposal algorithm [50] returns many boxes, only one of which is correct, we can use the bounding box estimator for people to assign each object proposal a score, as described in Section 3.2.1 and Equation 3.2. The box with the highest score is the box containing the person, which is the box we want to remove. The highest-scoring box was the correct box 100 percent of the time in our tests.

Once this box is located, we can replace all the pixels in that box with an interpolated color, the one that appears most frequently in the two pixels surrounding the outside of the proposed box borders. Two examples of correctly-interpolated frames are shown in Figure 4-12.

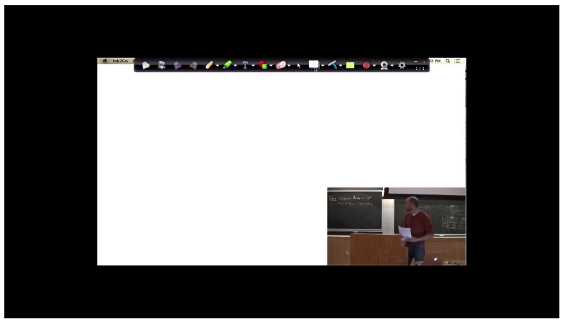

(a) Original frame

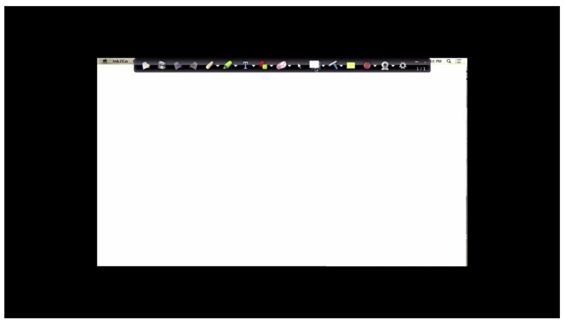

(b) Automatically interpolated

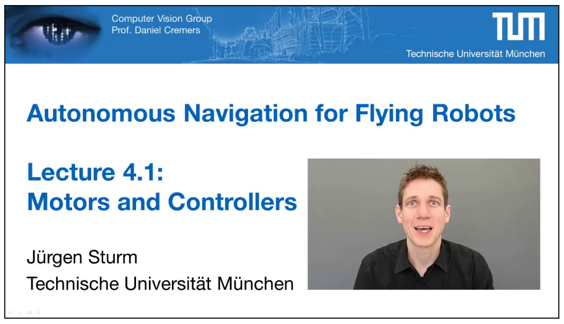

Autonomous Navigation for Flying Robots

Lecture 4.1:
Motors and Controllers

Jürgen Sturm
Technische Universität München

(c) Original frame

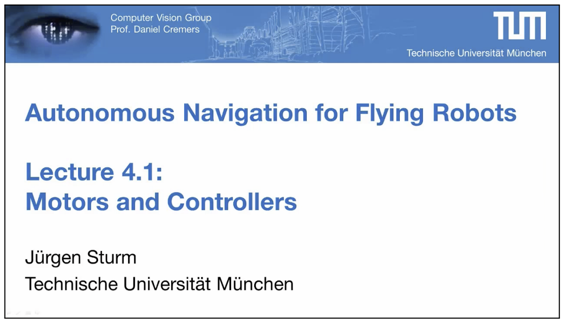

Autonomous Navigation for Flying Robots

Lecture 4.1:
Motors and Controllers

Jürgen Sturm
Technische Universität München

(d) Automatically interpolated

Figure 4-12: Two examples of picture-in-picture interpolation

However, in the failure case where the object proposal algorithm does not return the desired box, the system will automatically interpolate the wrong color, as shown in Figure 4-13. We rely on the fact that the videos are sampled every 5 frames and that the inner picture is fixed to take the majority-returned bounding box over many frames and take the bounding box returned by a local majority as the true bounding box for all frames.

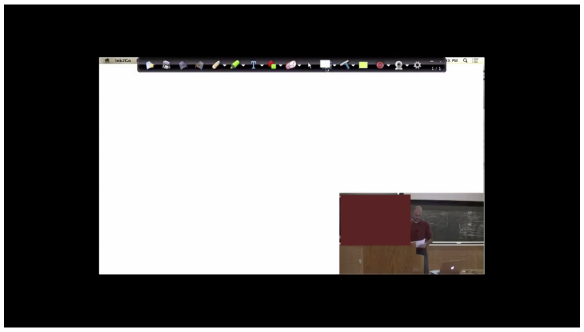

Figure 4-13: A potential interpolation failure caught by the local majority function at the end.

EdVidParse can be used to remove the inner picture from *picture-in-picture* video formats. In future work, the same principles can be extended to do lecturer subtraction and background blackboard interpolation, when combined with motion techniques for interpolating video frames [51].

Chapter 5

Discussion and Conclusion

5.1 Comparison of EdVidParse and R-CNN

We compare EdVidParse to the standard R-CNN system for object detection with two metrics in mind: accuracy and speed. R-CNN wins in accuracy, and EdVidParse wins in speed. In our baseline R-CNN system, we did not use bounding box regression like the original paper, and we used edge boxes [50] instead of selective search [41] for object proposal generation. The source code is for selective search closed-source, and it loses to edge boxes in both time and recall performance [19]. We did not use bounding box regression after classification because it offered no significant performance improvements for the two object classes tested.

While R-CNNs are on average more accurate, the EdVidParse method offers a significant performance speedup. For training, R-CNN takes 4 hours per class, while EdVidParse takes approximately 10 minutes per class. This offered more opportunity for training iterations in EdVidParse, perhaps contributing to improved results. For testing, EdVidParse offers a 100-fold speed improvement over R-CNN because EdVidParse requires only one forward-pass through the network while R-CNN requires nearly 1000. The AP score results are similar for R-CNN and EdVidParse, with R-CNN outperforming EdVidParse by a few percentage points. However, in practice, the speed of EdVidParse makes it more feasible to use over R-CNN. Tables 5.1 and 5.2 summarize the results.

	Person	Content
R-CNN	0.62	0.42
EdVidParse	0.439	0.434

Table 5.1: Best AP scores

	Train	Test
R-CNN	4 hours per class	30 seconds per frame
EdVidParse	10 minutes per class	$\leq$ 1 second per frame

Table 5.2: Average speed

5.2 Conclusion

EdVidParse provides a fast and easy way to extract people and content from educational videos, in addition to classifying the video production style in a given video frame. The techniques of using internal features to estimate bounding boxes work for small, specific datasets, even without cumbersome network fine-tuning. AP scores of more than 0.43 have been achieved for people and content, with manual tuning for a specific video yielding better results when necessary.

The three main design goals of speed, accuracy, and trainability are met, since EdVidParse improves almost 100-fold the speed at which R-CNN could accomplish the same task. However, while EdVidParse is accurate at acceptable levels, it is nowhere near perfect, and when used in practice should be combined with a manual sanity check. In practice, the ability to process lots of data with an initial first-pass with an automatic tool quickly is more useful than a slow tool that is more accurate. Because the proposed technique for bounding box estimation is a general technique that can be applied with limited training data, EdVidParse is flexible and easily re-trainable.

EdVidParse can now be used to correlate student interaction data with video events, as an input to a video viewing system that specially presents textual slide information to students, and in removing picture-in-picture video formats to just slides. Improvements to the model training procedure, including non-linear optimizations using simultaneous weighting and thresholding constraints, is also future work.

Educational videos are an increasing presence on the Internet, and EdVidParse can provide insights about the kinds of videos students are watching. Three case studies, classifying video production style, extracting people and textual content boxes, and removing the picture from picture-in-picture, have shown that EdVidParse is a useful tool in educational video analysis.

Appendix A

Figures

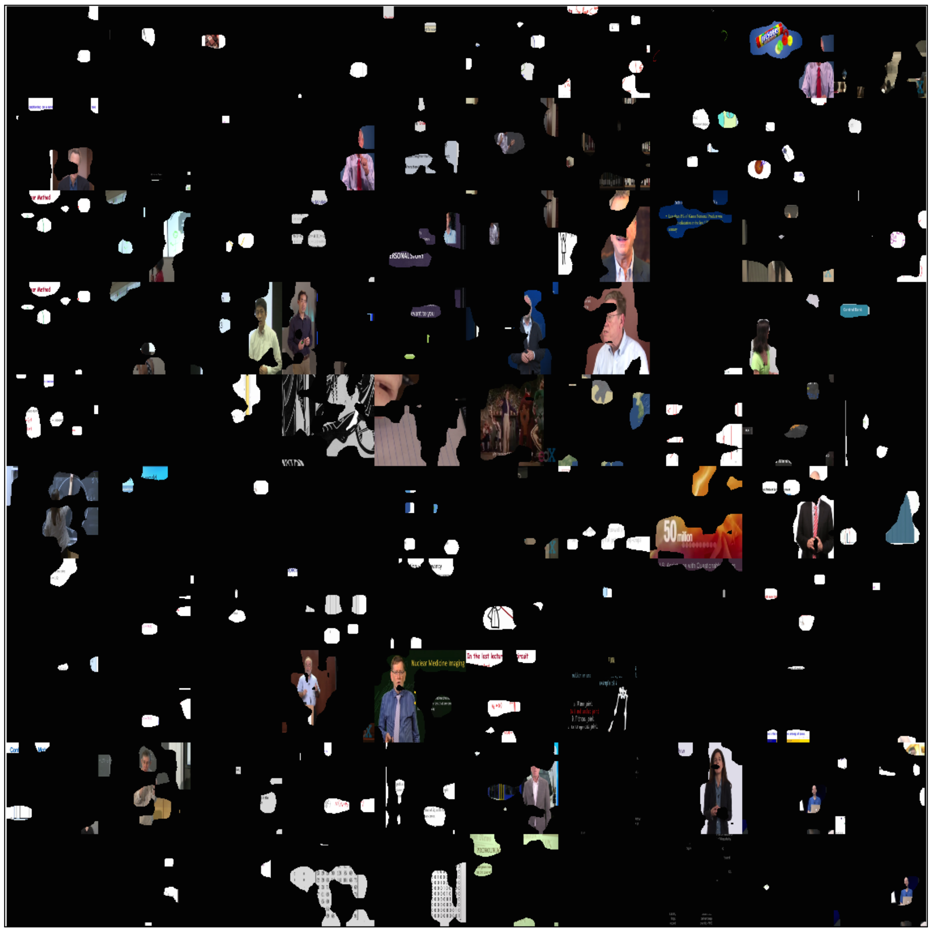

Figure A-1: Visualization of pool2, unit 39 activations. Used in person estimation.

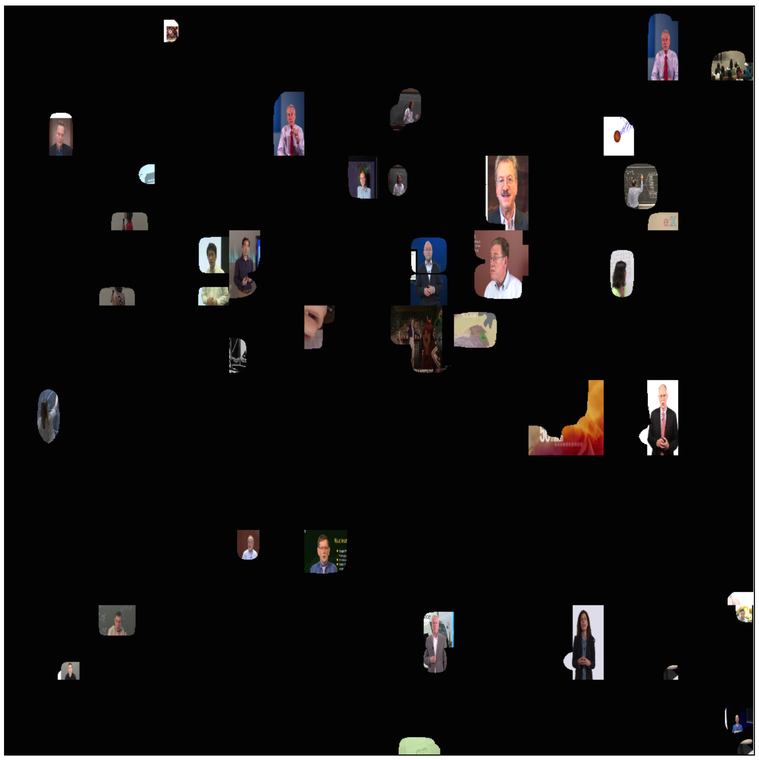

Figure A-2: Visualization of pool5, unit 3 activations. Used in person estimation.

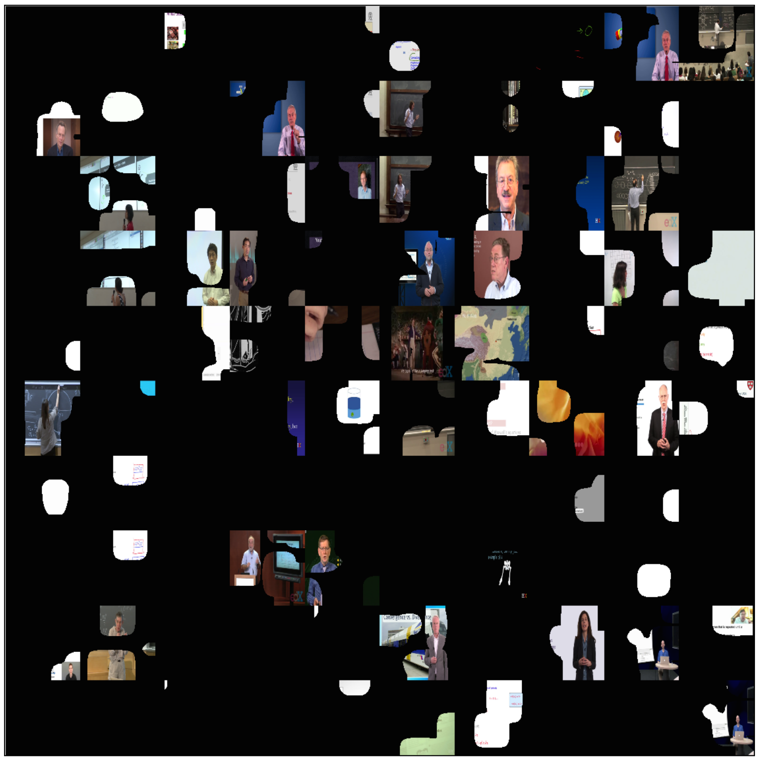

Figure A-3: Visualization of pool5, unit 199 activations. Used in person estimation.

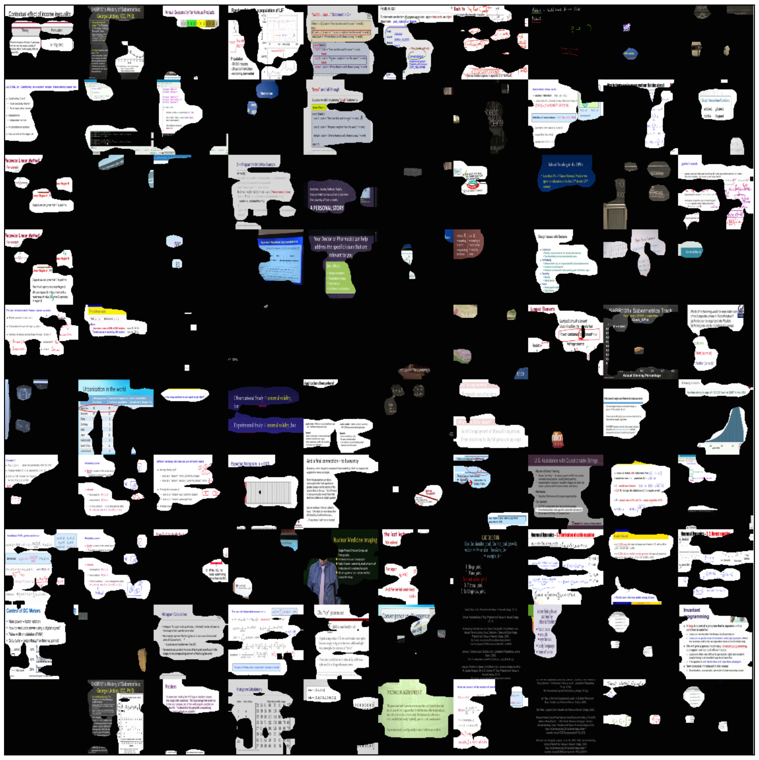
Figure A-4: Visualization of pool2, unit 134 activations. Used in content estimation.

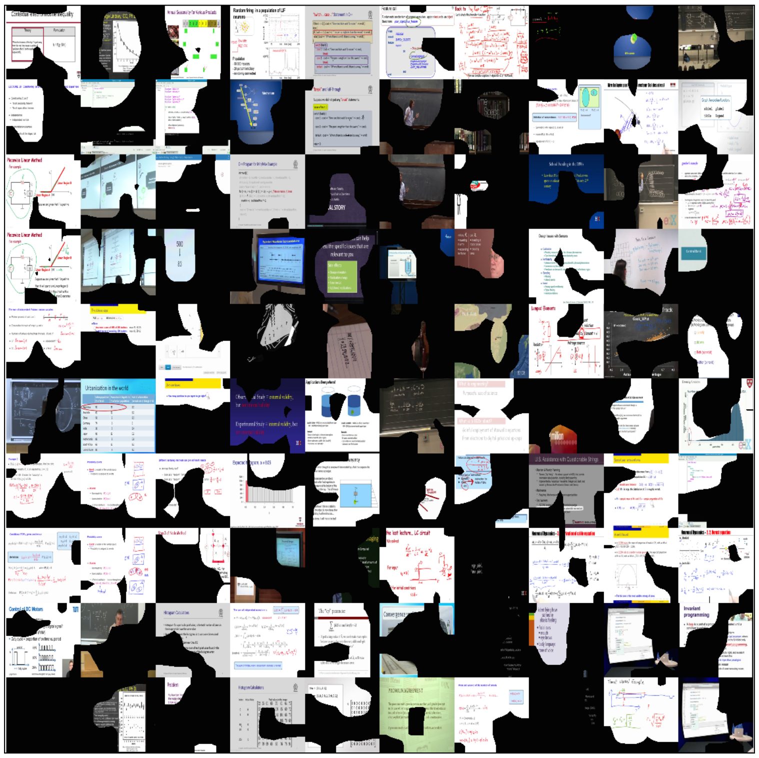
Figure A-5: Visualization of pool5, unit 251 activations. Used in content estimation.

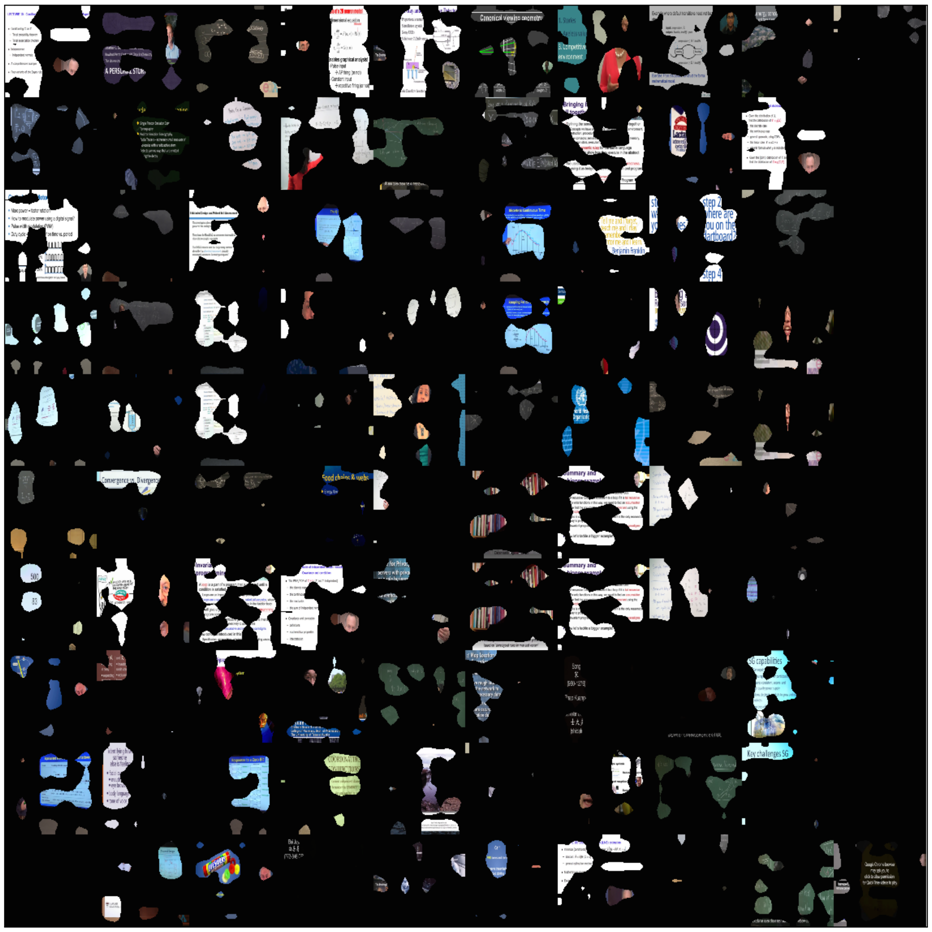
Figure A-6: Visualization of conv4, unit 174 activations. Used in content estimation.

Bibliography

[1] John Adcock, Matthew Cooper, Laurent Denoue, Hamed Pirsiavash, and Lawrence A. Rowe. TalkMiner: a search engine for online lecture video. In *Proceedings of the international conference on Multimedia*, pages 1507–1508. ACM, 2010.

[2] Pulkit Agrawal, Ross Girshick, and Jitendra Malik. Analyzing the performance of multilayer neural networks for object recognition. In *IEEE European Conference for Computer Vision (ECCV)*, pages 329–344. Springer, 2014.

[3] David Burns. Selenium, 2011.

[4] Chih-Chung Chang and Chih-Jen Lin. LIBSVM: a library for support vector machines. *ACM Transactions on Intelligent Systems and Technology (TIST)*, 2(3):27, 2011.

[5] Navneet Dalal and Bill Triggs. Histograms of oriented gradients for human detection. In *IEEE Conference on Computer Vision and Pattern Recognition (CVPR)*, volume 1, pages 886–893. IEEE, 2005.

[6] Jia Deng, Wei Dong, Richard Socher, Li-Jia Li, Kai Li, and Li Fei-Fei. Imagenet: A large-scale hierarchical image database. In *IEEE Conference on Computer Vision and Pattern Recognition (CVPR)*, pages 248–255. IEEE, 2009.

[7] Piotr Dollar and C. Lawrence Zitnick. Fast Edge Detection Using Structured Forests. *IEEE Transactions on Pattern Analysis and Machine Intelligence (PAMI)*, 2015.

[8] Piotr Dollár and C. Lawrence Zitnick. Structured forests for fast edge detection. In *Computer Vision (ICCV), 2013 IEEE International Conference on*, pages 1841–1848. IEEE, 2013.

[9] Jeff Donahue, Yangqing Jia, Oriol Vinyals, Judy Hoffman, Ning Zhang, Eric Tzeng, and Trevor Darrell. Decaf: A deep convolutional activation feature for generic visual recognition. In *Proceedings of the 31st International Conference on Machine Learning (ICML)*, pages 647–655, 2014.

[10] Dumitru Erhan, Christian Szegedy, Alexander Toshev, and Dragomir Anguelov. Scalable object detection using deep neural networks. In *Computer Vision*

and Pattern Recognition (CVPR), 2014 IEEE Conference on, pages 2155–2162. IEEE, 2014.

[11] Mark Everingham, Luc Van Gool, Christopher K. I. Williams, John Winn, and Andrew Zisserman. The Pascal Visual Object Classes (VOC) Challenge. *International Journal of Computer Vision*, 88(2):303–338, June 2010.

[12] Rong-En Fan, Kai-Wei Chang, Cho-Jui Hsieh, Xiang-Rui Wang, and Chih-Jen Lin. LIBLINEAR: A library for large linear classification. *The Journal of Machine Learning Research*, 9:1871–1874, 2008.

[13] P F Felzenszwalb, R B Girshick, D McAllester, and D Ramanan. Object Detection with Discriminatively Trained Part-Based Models. *IEEE Transactions on Pattern Analysis and Machine Intelligence*, 32(9):1627–1645, September 2010.

[14] Kunihiko Fukushima. Neocognitron: A self-organizing neural network model for a mechanism of pattern recognition unaffected by shift in position. *Biological cybernetics*, 36(4):193–202, 1980.

[15] Michael A. Gelbart, Jasper Snoek, and Ryan P. Adams. Bayesian optimization with unknown constraints. In *Uncertainty in Artificial Intelligence*, 2014.

[16] Ross Girshick, Jeff Donahue, Trevor Darrell, and Jitendra Malik. Rich feature hierarchies for accurate object detection and semantic segmentation. In *IEEE Conference on Computer Vision and Pattern Recognition (CVPR)*, 2014.

[17] Xavier Glorot and Yoshua Bengio. Understanding the difficulty of training deep feedforward neural networks. In *International Conference on Artificial Intelligence and Statistics*, pages 249–256, 2010.

[18] Philip J. Guo, Juho Kim, and Rob Rubin. How video production affects student engagement: an empirical study of MOOC videos. In *Proceedings of the first ACM conference on Learning @ Scale*, pages 41–50. ACM Press, 2014.

[19] Jan Hosang, Rodrigo Benenson, Piotr Dollár, and Bernt Schiele. What makes for effective detection proposals? *arXiv preprint arXiv:1502.05082*, 2015.

[20] Sara T. Itani. *EduCase: an automated lecture video recording, post-processing, and viewing system that utilizes multimodal inputs to provide a dynamic student experience.* Masters of Engineering, Massachusetts Institute of Technology, 2013.

[21] Yangqing Jia, Evan Shelhamer, Jeff Donahue, Sergey Karayev, Jonathan Long, Ross Girshick, Sergio Guadarrama, and Trevor Darrell. Caffe: Convolutional Architecture for Fast Feature Embedding. *arXiv preprint arXiv:1408.5093*, 2014.

[22] Esha Baidya (Kayal). LectureKhoj: Automatic tagging and semantic segmentation of online lecture videos. *2014 Seventh International Conference on Contemporary Computing (IC3)*, pages 37–43, August 2014.

[23] Juho Kim, Philip J. Guo, Daniel T. Seaton, Piotr Mitros, Krzysztof Z. Gajos, and Robert C. Miller. Understanding In-Video Dropouts and Interaction Peaks in Online Lecture Videos. In *Proceedings of the first ACM conference on Learning @ Scale*, pages 31–40, 2014.

[24] Kazuaki Kishida. Property of Average Precision and its Generalization: An Examination of Evaluation Indicator for Information Retrieval Experiments. NII Technical Report NII-2005-014E, National Institute of Informatics, Tokyo, Japan, October 2005.

[25] René F. Kizilcec, Kathryn Papadopoulos, and Lalida Sritanyaratana. Showing face in video instruction: effects on information retention, visual attention, and affect. In *Proceedings of the 32nd annual ACM conference on Human factors in computing systems*, pages 2095–2102. ACM Press, 2014.

[26] Alexander Klaser, Marcin Marszalek, and Cordelia Schmid. A spatio-temporal descriptor based on 3d-gradients. In *BMVC 2008-19th British Machine Vision Conference*, pages 275–1. British Machine Vision Association, 2008.

[27] Alex Krizhevsky, Ilya Sutskever, and Geoffrey E. Hinton. Imagenet classification with deep convolutional neural networks. In *Advances in neural information processing systems*, pages 1097–1105, 2012.

[28] Rebecca Krosnick. *VideoDoc: Combining Videos and Lecture Notes for a Better Learning Experience.* Masters of Engineering, MIT, 2015.

[29] Yann LeCun, B. Boser, J. S. Denker, D. Henderson, and L. D. Jackel. Backpropagation Applied to Handwritten Zip Code Recognition Y. LeCun. *Neural Computation*, 1(4):541–551, 1989.

[30] David G. Lowe. Distinctive image features from scale-invariant keypoints. *International journal of computer vision*, 60(2):91–110, 2004.

[31] Aude Oliva and Antonio Torralba. Modeling the shape of the scene: A holistic representation of the spatial envelope. *International journal of computer vision*, 42(3):145–175, 2001.

[32] Amy Pavel, Colorado Reed, Björn Hartmann, and Maneesh Agrawala. Video digests: a browsable, skimmable format for informational lecture videos. In *Proceedings of the 27th annual ACM symposium on User interface software and technology*, pages 573–582. ACM Press, 2014.

[33] David E. Rumelhart, Geoffrey E. Hinton, and Ronald J. Williams. Learning internal representations by error propagation. In David E. Rumelhart and James L. McClelland, editors, *Parallel Distributed Processing: Explorations in the Microstructure of Cognition*, volume I, pages 318–362. Bradford Books, Cambridge, Mass., 1986.

[34] Olga Russakovsky, Jia Deng, Hao Su, Jonathan Krause, Sanjeev Satheesh, Sean Ma, Zhiheng Huang, Andrej Karpathy, Aditya Khosla, Michael Bernstein, and others. ImageNet Large Scale Visual Recognition Challenge (ILSVRC). *arXiv preprint arXiv:1409.0575*, 2014.

[35] Kshitij Sharma, Patrick Jermann, and Pierre Dillenbourg. How Students Learn using MOOCs: An Eye-tracking Insight. In *EMOOCs 2014, the Second MOOC European Stakeholders Summit*, 2014.

[36] Jasper Snoek. *Bayesian Optimization and Semiparametric Models with Applications to Assistive Technology*. PhD thesis, University of Toronto, 2013.

[37] Jasper Snoek, Hugo Larochelle, and Ryan P. Adams. Practical Bayesian optimization of machine learning algorithms. In *Advances in Neural Information Processing Systems*, pages 2951–2959, 2012.

[38] Jasper Snoek, Kevin Swersky, Richard S. Zemel, and Ryan P. Adams. Input warping for Bayesian optimization of non-stationary functions. In *International Conference on Machine Learning*, 2014.

[39] Kah-Kay Sung and Tomaso Poggio. Example-based learning for view-based human face detection. *Pattern Analysis and Machine Intelligence, IEEE Transactions on*, 20(1):39–51, 1998.

[40] Kevin Swersky, Jasper Snoek, and Ryan P. Adams. Multi-task bayesian optimization. In *Advances in Neural Information Processing Systems*, pages 2004–2012, 2013.

[41] J. R. R. Uijlings, K. E. A. van de Sande, T. Gevers, and A. W. M. Smeulders. Selective Search for Object Recognition. *International Journal of Computer Vision*, 104(2):154–171, September 2013.

[42] Yuanyuan Wang, Yukiko Kawai, and Kazutoshi Sumiya. An Exploratory Search for Presentation Contents based on Slide Semantic Structure. In *Proc. of the 26th International Conference on Software Engineering and Knowledge Engineering (SEKE 2014)*, pages 665–670, July 2014.

[43] Sarah Weir, Juho Kim, Krzysztof Z. Gajos, and Robert C. Miller. Learnersourcing Subgoal Labels for How-to Videos. pages 405–416. ACM Press, 2015.

[44] Jianxiong Xiao, Krista A. Ehinger, James Hays, Antonio Torralba, and Aude Oliva. SUN Database: Exploring a Large Collection of Scene Categories. *International Journal of Computer Vision*, August 2014.

[45] Haojin Yang, Maria Siebert, Patrick Luhne, Harald Sack, and Christoph Meinel. Lecture Video Indexing and Analysis Using Video OCR Technology. In *Signal-Image Technology and Internet-Based Systems (SITIS), 2011 Seventh International Conference on*, pages 54–61. IEEE, November 2011.

[46] Jason Yosinski, Jeff Clune, Yoshua Bengio, and Hod Lipson. How transferable are features in deep neural networks? In *Advances in Neural Information Processing Systems*, pages 3320–3328, 2014.

[47] Hong Qing Yu, C. Pedrinaci, S. Dietze, and J. Domingue. Using Linked Data to Annotate and Search Educational Video Resources for Supporting Distance Learning. *IEEE Transactions on Learning Technologies*, 5(2):130–142, April 2012.

[48] Bolei Zhou, Aditya Khosla, Agata Lapedriza, Aude Oliva, and Antonio Torralba. Object Detectors Emerge in Deep Scene CNNs. In *3rd International Conference on Learning Representations (ICLR)*, 2015.

[49] Bolei Zhou, Agata Lapedriza, Jianxiong Xiao, Antonio Torralba, and Aude Oliva. Learning Deep Features for Scene Recognition using Places Database. In *Advances in Neural Information Processing Systems (NIPS)*, 2014.

[50] C. Lawrence Zitnick and Piotr Dollár. Edge boxes: Locating object proposals from edges. In *IEEE European Conference for Computer Vision (ECCV)*, pages 391–405, 2014.

[51] C. Lawrence Zitnick, Sing Bing Kang, Matthew Uyttendaele, Simon Winder, and Richard Szeliski. High-quality video view interpolation using a layered representation. In *ACM Transactions on Graphics (TOG)*, volume 23, pages 600–608. ACM, 2004.